Check for updates

New Zealand Journal of Geology and Geophysics

RESEARCH ARTICLE OPEN ACCESS

Evolution of the Transantarctic Basin (Southern Gondwana): Insights From Quantitative Sandstone Petrography

Luca Zurli[1,2] | Marco Fioraso[1] | Matteo Perotti[1] | Andrea Di Giulio[3] | Valerio Olivetti[4] | Samuele Pezzoli[3] | Valentina Corti[1,2] | Gianluca Cornamusini[1,2]

[1]Department of Physical Sciences, Earth and Environment, University of Siena, Siena, Italy | [2]National Museum of Antarctica – Siena Section, University of Siena, Siena, Italy | [3]Department of Earth and Environmental Sciences, University of Pavia, Pavia, Italy | [4]Department of Geosciences, University of Padova, Padova, Italy

Correspondence: Luca Zurli (luca.zurli@unisi.it)

Received: 25 April 2025 | **Revised:** 17 October 2025 | **Accepted:** 21 October 2025

Keywords: Antarctica | Beacon Supergroup | foreland basin | Gondwana | Parmeener Supergroup | Tasmania

ABSTRACT

The deposition of the sandstone sedimentary succession of the Beacon Supergroup lasted more than 200 Myr (Devonian to Early Jurassic) in Victoria Land and nearby territories in the so-called Transantarctic Basin, recording crucial events in the history of the Earth. Sedimentation is synchronous with the convergence between the paleo-Pacific plate and Gondwana, to form the large Gondwanide orogenic system. The composition of the Beacon Supergroup sandstones was found to be correlated with major tectonic processes in response to subduction dynamics, which ultimately conditioned the source-to-sink system and provenance imprints. Petrographic variability in sandstone composition is tracked through space and time by a quantitative analysis of all available published data and new updated ones, from the Transantarctic Mountains and Tasmania. The variability of grain composition detected by quantitative sandstone petrography reveals that the Victoria Land sector transitioned from an intracratonic basin in back-bulge position to a foredeep basin setting.

1 | Introduction

The study of the sedimentary record allows us to understand the Earth's dynamics in the deep past, reconstructing the depositional environments, the climate conditions, and contributing to understand the continental and geodynamic plate assemblages. Long-lasting active convergent margins tend to increase topography and crust thickness by accretion at the boundary between continental and oceanic lithospheres, thrusting, and magmatic emplacement. The orogenic wedge loads the lithosphere causing an increase in accommodation space due to flexural subsidence (Beaumont 1981; DeCelles and Giles 1996), filled by orogen-derived sediments. Basin depozones are located on both sides of the orogeny, forming forearc and retroarc foreland basins (sensu DeCelles 2012; Allen and Allen 2013). The retroarc foreland systems refer to two main depocenters, the foredeep and the back-bulge basins, and a high induced by flexure, the peripheral bulge (DeCelles and Giles 1996; DeCelles 2012). Subsidence and uplift in each sector of the basin depend on the interplay between tectonic loading and sub-lithospheric processes, resulting in physical changes of the depositional system (Catuneanu 2004).

In addition, the compositional characterization of sedimentary sequences allows for depiction of the geological evolution of an orogen even after the nearly-complete erasing and exposure of its hidden roots (Graham et al. 1986; Jordan et al. 1988; Critelli 2018; Critelli et al. 2023; Zhang et al. 2025). During the Late Paleozoic to Mesozoic, convergence occurred between the East Antarctic lithosphere and the paleo-Pacific Ocean in southern Gondwana leading the development of the Gondwanide Orogeny (Goodge 2020 and

This is an open access article under the terms of the Creative Commons Attribution License, which permits use, distribution and reproduction in any medium, provided the original work is properly cited.

© 2026 The Author(s). *New Zealand Journal of Geology and Geophysics* published by John Wiley & Sons Australia, Ltd on behalf of Royal Society of New Zealand Te Apārangi.

reference therein), and widespread sedimentary basins were filled by thick clastic sequences fed by both mountain belts and cratonic terranes (Collinson et al. 1994; Elliot 2013, Forsyth 1989).

Even if the Gondwanide Orogeny developed since the latest Carboniferous up to the earliest Jurassic along the southern Gondwana margin, it is poorly documented and limited to Antarctic Peninsula and eastern Marie Byrd Land (Pankhurst et al. 1993) because of the Mesozoic Gondwana breakup and Cenozoic erosion and glacial cover. In that scenario, the sequences that filled the sedimentary basins offer the best opportunity to unveil the geodynamic evolution of this plate margin portion. The tectonic activity related to geodynamic evolution causes differences in the sediment infilling composition. Therefore, the quantitative petrographic investigation of sandstones through time and space allows us to define the main timesteps defining the Gondwanide Orogeny.

Since the Devonian up to Early Jurassic, sedimentary basins recorded the evolution of multiple orogenetic phases since craton erosion to the beginning of accretionary events, the increasing topographic building and later stages of tectonic inversion before the start of Gondwana supercontinent fragmentation. The Transantarctic Basin is one of the least explored foreland system due to its remote location and limited outcrop exposure because of the ice cover, even though it records an extremely complex and interesting depositional history of a large region of the Earth's surface. In fact, the Transantarctic and Tasmania basins record within their sedimentary strata the long-lasting evolution of the Paleo-Pacific slab subduction and southern Gondwana orogenic belts (Figure 1; Glen & Cooper 2021) and the emplacement of the Ferrar Large Igneous Province (Elliot and Fleming 2021 and reference therein).

The Transantarctic Basin was geotectonically interpreted in different ways as: foreland basin (Dalziel and Elliot 1982; Collinson 1990; Collinson et al. 1994; Elliot 2013; Zurli et al. 2024a); distal foreland flexure (Woolfe and Barrett 1995); craton tilting (Mitrovica et al. 1989); and intracratonic basin (Barrett 1981, 1991; Woolfe and Barrett 1995). The Tasmania Basin geotectonic interpretation is also debated as a foreland basin (Collinson et al. 1987; Fielding et al. 2010) or as an intracratonic basin (Veevers et al. 1994).

This work aims to show how quantitative detrital petrography could be an important tool to study an active plate margin, to define the spatial–temporal evolution of an orogenic belt through the study

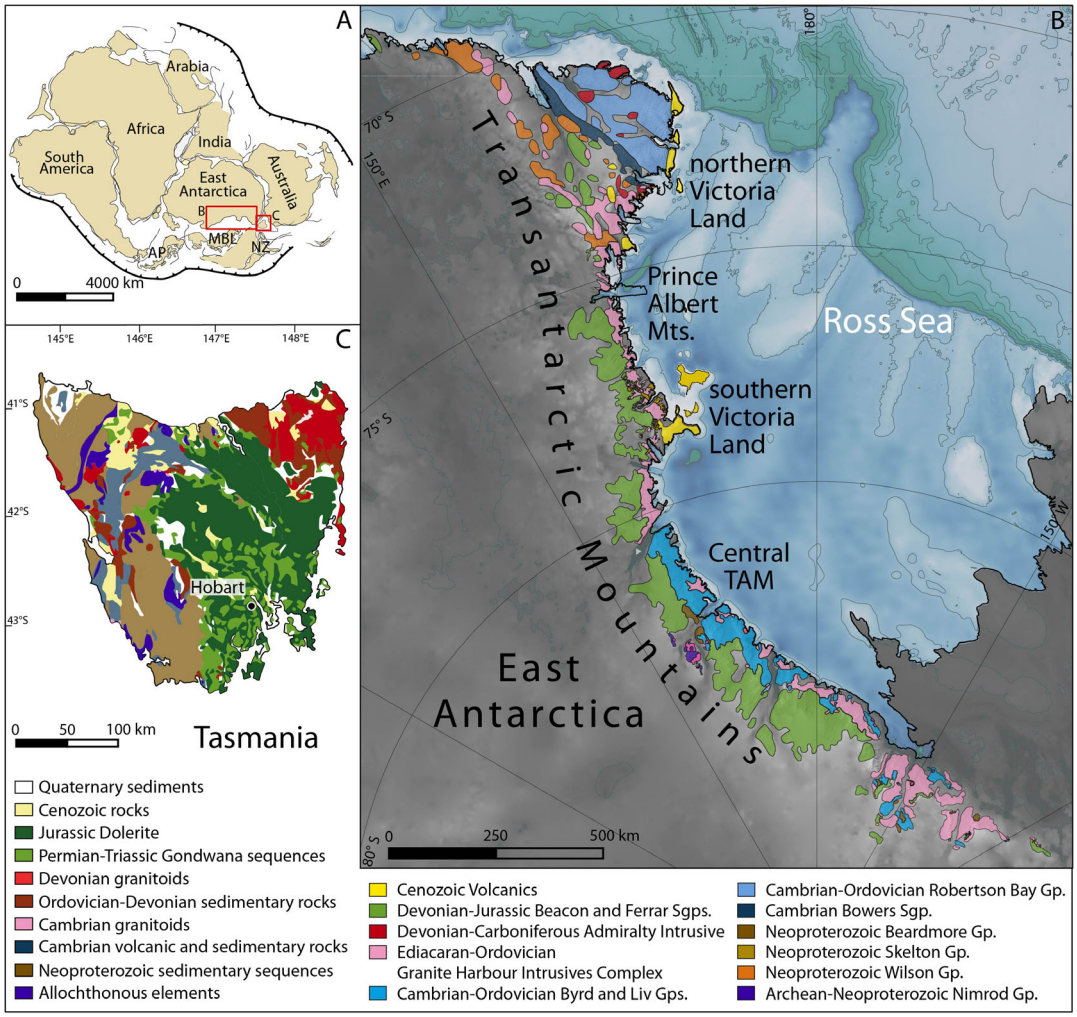

FIGURE 1 | (A) Continental block assemblage of Gondwana supercontinent in the Permian (modified from Sirevaag et al. 2018). Study areas are shown. AP: Antarctic Peninsula, MBL: Marie Byrd Land, NZ: New Zealand; (B) simplified geological map of the Transantarctic Mountains (modified from Cox et al. 2023). Topography and bathymetry are from BedMachine Antarctica V3 (Morlighem et al. 2020 and Morlighem 2022); and (C) simplified geological map of Tasmania (modified from Brown et al. 1995; Stacey and Berry 2004).

11758791, 2026, 1, Downloaded from https://nzjg.onlinelibrary.wiley.com/doi/10.1002/jgo2.70023 by CochraneItalia, Wiley Online Library on [10/03/2026]. See the Terms and Conditions (https://onlinelibrary.wiley.com/terms-and-conditions) on Wiley Online Library for rules of use; OA articles are governed by the applicable Creative Commons License

sediments deriving from its dismantling. Different models can coexist through time and space, and gradual transition between diverse tectonic settings occurred, reflecting the spatial–temporal evolution of the Gondwanide orogenic system. To achieve this objective, it was necessary to conduct a thorough review of the many and varied compositional data on sandstones published over time, homogenizing, revising, and integrating them with new original data, with a view to placing them within a macroregional geological framework that is homogeneous in time and space and consistent with the most recent provenance and geodynamic models.

2 | Geological Setting

2.1 | Regional Geology

During the Paleozoic, East Antarctica and Tasmania blocks occupied the proto-Pacific margin of Gondwana and they experienced a common geological evolution (Figure 1). These regions were involved in the Early Paleozoic Ross-Tyennan-Delamerian Orogeny, followed by the Middle Paleozoic orogenic activity; since the Permian, these regions have hosted sedimentary basins developed within the Gondwanide Orogeny system.

The basement exposed in the Transantarctic Mountains (TAM) is constituted mostly by the Neoproterozoic-Early Paleozoic Ross Orogenic belt and, in a minor part, by the Precambrian craton and Neoproterozoic passive margin meta-sediments (Figure 1). From ~550 to ~480 Ma (Goodge 2020; Glen and Cooper 2021), subduction-related igneous rocks occurred as granitic batholiths, belonging to the Granite Harbor Intrusive Complex, across all the active margin with the Paleo-Pacific plate. The intrusive rocks show high compositional variability along the belt (Gunner 1971; Cox et al. 2012; Kim et al. 2021). At the same time span, the continental-arc collision led to the Tyennan Orogeny in Tasmania, with granites that intruded the deformed Precambrian meta-sedimentary units (Figure 1; Corbet et al. 2014).

The metamorphic and igneous rocks formed during the Ross Orogeny in East Antarctica were subsequently uplifted and eroded in the Ordovician and Silurian leading to the development of a regional-scale flat-lying surface, the Kukri Erosion Surface (McKelvey et al. 1977). In the Devonian, southern Victoria Land (SVL) and central TAM hosted an intracratonic basin where the Beacon Supergroup deposition started in a mainly continental to shallow marine environment forming, the Taylor Group strata (Cox et al. 2012; Bradshaw 2013). On the contrary, deposition occurred in Tasmania during the Ordovician and Silurian: in eastern Tasmania, thick turbiditic sequences, the Mathinna Supergroup, formed; in western Tasmania postorogenic shallow marine siliciclastic and carbonate successions, the Gordon and Eldon groups, were deposited (Calver et al. 2014 and references therein). Since the Devonian deformation of the Tabberabberan Orogeny involved Tasmania, with magmatism dated between ca. 400–374 Ma in eastern Tasmania, and ca. 373–351 Ma in western Tasmania (Seymour et al. 2014). Magmatic activity in a back arc setting is also recorded in East Antarctica with the emplacement of the Admiralty Intrusives and Gallipoli Volcanics occurring in northern Victoria Land (NVL, Kreuzer et al. 1987; Glen and Cooper 2021; Talarico et al. 2022 and references therein) and West Antarctica with the Ford Granodiorite in Marie Byrd Land (Pankhurst et al. 1998; Yakymchuk et al. 2015).

After the Devonian deformational and magmatic activities, both Tasmania and East Antarctica experienced a prolonged erosional phase that led to the formation of the Great Unconformity in Tasmania and of the Maya Erosion Surface in Antarctica. Above those, started the deposition of the Gondwana sequences: the Victoria Group of the Beacon Supergroup in the Transantarctic Basin and the Parmeener Supergroup in the Tasmania Basin. The basins formed in a retroarc setting of the Gondwanide Orogeny, led by the slab subduction of the paleo-Pacific plate under Gondwana margin. Remnants of the arc occur in West Antarctica and Antarctic Peninsula, while deformation of the fold and thrust belt are recorded in the Ellsworth Mountains (Boger 2011). Gondwana sequences deposition lasted until the Early Jurassic when the Ferrar Large Igneous Province was emplaced in East Antarctica, Tasmania, and Australia (Elliot and Fleming 2021).

2.2 | Gondwana Sequences Stratigraphy

The Beacon Supergroup in the Transantarctic Basin is subdivided into the Devonian Taylor and the Permian-Jurassic Victoria groups (Figure 2). The Parmeener Supergroup in the Tasmania Basin is divided into a lower part, representing the Permian deposition in a glacial and marine environment, and an upper part representing the latest Permian to Triassic continental deposition (Figure 2; Forsyth 1989).

The Devonian Taylor Group represents deposition in an epicratonic basin, the McMurdo Basin (Bradshaw 2013), reaching the maximum thickness of ca. 1400 m in the Dry Valleys region in SVL, where the depocenter of the basin was placed. The thickness gently decreases southward, up to the Shackleton Glacier in central TAM (CTAM), while it steeply decreases northward, and the basin margin was in southern Prince Albert Mountains (PAM; Olivetti et al. 2026; Corti et al. 2026, under review), with absence of the Devonian strata in NVL and Tasmania. In SVL, the Taylor Group is divided into 8 formations (Figure 2). The depositional environment of the lower part of the Taylor Group is debated between alluvial and shallow-marine settings (see Cox et al. 2012), while the upper formations, Beacon Heights Orthoquartzite and Aztec Siltstones are respectively deposited in a low-sinuosity braided rivers with subaerial exposures (Barrett et al. 1971; Barrett and Webb 1973; Barrett and Kohn 1975) and an alluvial plain (McPherson 1978).

The Taylor and Victoria groups are then separated by an unconformity, the Maya Erosion Surface, marking a significant stratigraphic gap. The deposition of the Victoria Group began in the Late Carboniferous(?)-Early Permian with the glacigenic sedimentation related to the Late Paleozoic Ice Age. These deposits represent sedimentation in an ice proximal to distal subaqueous glacial environment, and their distribution is not homogeneous, infilling the paleo-morphological lows, where the ice caps and tongues flowed (Isbell et al. 2008; Isbell 2010; Koch and Isbell 2013; Cornamusini et al. 2017; Ives and Isbell 2021; Zurli et al. 2022a, 2022b). The Tasmania Basin recorded the deposition of thick glaciomarine sequences that filled the morphological lows (Forsyth 1989; Fielding et al. 2010; Henry et al. 2012; Zurli et al. 2022a; Ives and Isbell 2023). Following the glacial retreat during the Permian, the basin in CTAM and Victoria Land experienced the instauration of alluvial systems, characterized by sandy braided to anastomosed fluvial systems in a richly

11758791, 2026, 1, Downloaded from https://nzjg.onlinelibrary.wiley.com/doi/10.1002/jgg2.70023 by CochraneItalia, Wiley Online Library on [10/03/2026]. See the Terms and Conditions (https://onlinelibrary.wiley.com/terms-and-conditions) on Wiley Online Library for rules of use; OA articles are governed by the applicable Creative Commons License

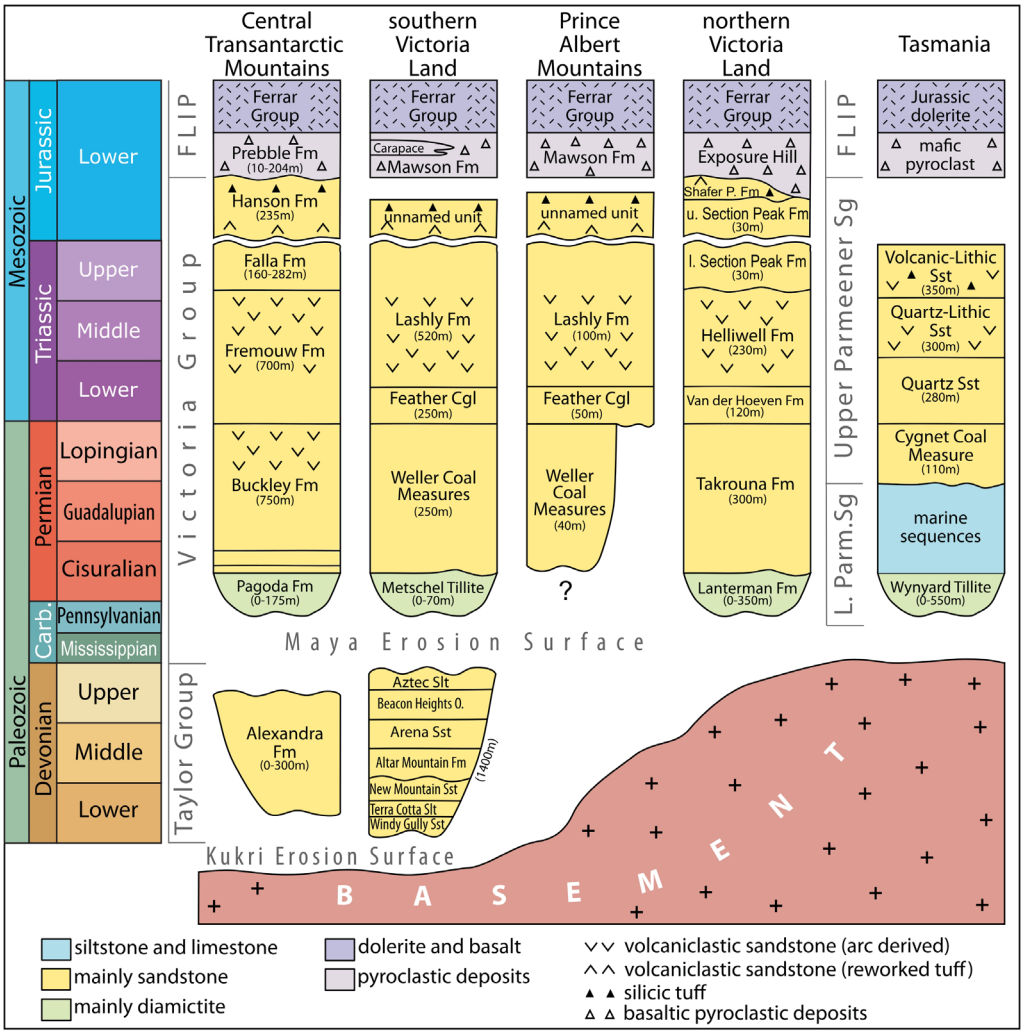

FIGURE 2 | Simplified stratigraphic scheme of the southern Gondwana sequences in the studied areas. Stratigraphy is adapted from Elliot (2013), Reid et al. (2014), Elliot et al. 2017a, 2017b), Cornamusini et al. (2017, 2023), Bomfleur et al. (2021), Zurli et al. (2022a, 2022b); Olivetti et al. 2026; Corti et al. 2026 (under review). Bracket numbers represent the estimated thickness of the formations. FLIP: Ferrar Large Igneous Province, Fm: Formation, Slt: Siltstone, Sst: Sandstone, O: Orthoquartzite.

vegetated floodplain (Isbell et al. 1997). These latter characterized the Transantarctic Basin during the Late Permian, leading to the deposition of sandstone strata interlayered with carbonaceous mudstone and coal (Isbell & Cúneo 1996; Cornamusini et al. 2023). On the contrary, at the same time, the Tasmania Basin recorded marine deposition (Figure 2; Fielding et al. 2010; Reid et al. 2014). At the end of the Permian, Earth's climate experienced an abrupt change, likely triggered by the emplacement of the Siberian Trap combined with a contribution of other global-scale geodynamic processes (Svensen et al. 2009; Burgess et al. 2017; Dal Corso et al. 2022; Di Giulio et al. 2026), leading to the largest mass extinction. In the continental environment of southern Gondwana, the terrestrial mass extinction was recorded in the Beacon Supergroup deposits (Retallack et al. 2005; Cornamusini et al. 2023; Sidor et al. 2023), as well in the Sydney Basin deposits (Fielding et al. 2019). Above the Permian-Triassic boundary, sedimentary sequences are characterized by the instauration of a braided fluvial system in a nonvegetated floodplain in the Transantarctic and Tasmania basins (Barrett and Fitzgerald 1985; Barrett 1991; Collinson et al. 1994; Reid et al. 2014; Cornamusini et al. 2023). The deposition in the Triassic was then characterized by the alternation of meandering and braided fluvial systems that cut vegetated floodplains (Barrett 1991; Collinson et al. 1994; Reid et al. 2014; Cornamusini et al. 2023); the result is the abundance of coal beds, fossil leave impressions, and silicified woods in the Triassic deposits (Gulbranson et al. 2020).

Between the end of the Triassic and the Early Jurassic, the geodynamic setting transitioned from a convergent active margin to the extension and breakup of Gondwana. Prior to the emplacement of the mafic products of Ferrar Large Igneous Province, several silicic volcaniclastic beds are largely sparse among Beacon Supergroup strata (Figure 2; Elliot et al. 2017b). The felsic volcanic products are synchronous with the emplacement of the Chon Aike magmatic province that crops out in the Ellsworth-Whitmore Mountains, Antarctic Peninsula, and South America (Craddock et al. 2017b; Bastias et al. 2021; Riley et al. 2023). After that, flood lavas and pyroclastic rocks invaded the alluvial depositional basin interfingering at the beginning and then ending the continental sedimentation (Casnedi and Di Giulio 1999), whereas dolerite sills and dykes emplaced into basement rock and the Beacon Supergroup sedimentary sequence (Elliot and Fleming 2021 and references therein).

11758791, 2026, 1, Downloaded from https://nzjg.onlinelibrary.wiley.com/doi/10.1002/jgo2.70023 by CochraneItalia, Wiley Online Library on [10/03/2026]. See the Terms and Conditions (https://onlinelibrary.wiley.com/terms-and-conditions) on Wiley Online Library for rules of use; OA articles are governed by the applicable Creative Commons License

3 | Material and Methods

This work combines more than 680 sandstone quantitative petrography data (Table S1) from literature and new data from samples collected in Tasmania outcrops and borehole (Table 1). Tables reporting the point-counting data were acquired and literature data have been reorganized and recalculated to obtain a homogeneous framework to build up compositional ternary diagrams (i.e., Quartz—Feldspars—Rock Fragments). The ternary diagrams were plotted following McBride (1963), where quartz (Q) pole includes monocrystalline and polycrystalline quartz, feldspar (F) pole includes monocrystalline feldspars grains, and rock fragment (Rf) pole includes fine- and coarse-grained

TABLE 1 | The table summarizes the samples used in this article and their distribution through space and time.

Region	Group	Formation	Age	Samples	References
CTAM	Taylor	Alexandra Fm.	Devonian	7	(Barrett et al. 1986)
CTAM	Victoria	Pagoda Tillite	L. Carb. - E. Permian	7	(Barrett et al. 1986)
CTAM	Victoria	Mackellar Fm.	E. Permian	8	(Barrett et al. 1986)
CTAM	Victoria	Fairchild Fm.	E. Permian	26	(Barrett et al. 1986)
CTAM	Victoria	Buckley Fm.	Permian	62	(Barrett et al. 1986; Sidor et al. 2023)
CTAM	Victoria	Fremouw Fm.	Triassic	66	(Barrett et al. 1986; Sidor et al. 2023)
CTAM	Victoria	Falla Fm.	L. Triassic	18	(Barrett et al. 1986)
SVL	Taylor	Beacon Heights O.	Devonian	4	(Korsch 1974)
SVL	Taylor	Arena Sst.	Devonian	3	(Korsch 1974)
SVL	Taylor	Altair Mountains S.	Devonian	7	(Korsch 1974)
SVL	Taylor	Aztec Siltstone	Devonian	12	(McPherson 1975)
SVL	Victoria	Metschel Tillite	L. Carb. - E. Permian	9	(Zurli 2018)
SVL	Victoria	Weller Coal Measures	Permian	28	(Korsch 1974; Collinson et al. 1983; Cornamusini et al. 2023; Zurli et al. 2024a)
SVL	Victoria	Feather Conglomerate	E. Triassic	18	(Korsch 1974; Collinson et al. 1983; Cornamusini et al. 2023; Zurli et al. 2024a)
SVL	Victoria	Lashly Fm.	Triassic	86	(Korsch 1974; Collinson et al. 1983; Cornamusini et al. 2023; Zurli et al. 2024a)
PAM	Victoria	Weller Coal Measures	Permian	7	(Olivetti et al. 2026)
PAM	Victoria	Feather Conglomerate	E. Triassic	9	(Bernet and Gaupp 2005; Olivetti et al. 2026)
PAM	Victoria	Lashly Fm.	Triassic	27	(Bernet and Gaupp 2005; Olivetti et al. 2026)
PAM	Victoria	Lashly Fm. - unnamed unit	L. Triassic - E. Jurassic	11	(Bernet and Gaupp 2005; Olivetti et al. 2026)
NVL	Victoria	Lanterman Fm.	L. Carb. - E. Permian	13	(Cornamusini et al. 2017; Zurli 2018)
NVL	Victoria	Takrouna Fm	Permian	53	(Collinson et al. 1986)
NVL	Victoria	Van der Hoeven Fm	E. Triassic	4	(Bomfleur et al. 2021)
NVL	Victoria	Helliwell Fm	Triassic	3	(Bomfleur et al. 2021)
NVL	Victoria	Section Peak Fm.	L. Triassic - E. Jurassic	81	(Collinson et al. 1986; Di Giulio et al. 1999; Bomfleur et al. 2021)
TAS	upper Parmeener	Cygnet Coal Measures	Permian	18	this paper
TAS	upper Parmeener	Quartz Sandstone	E. Triassic	72	(Collinson et al. 1990); this paper
TAS	upper Parmeener	Quartz and Lithic Sandstone	Triassic	28	(Collinson et al. 1990)

11758791, 2026, 1, Downloaded from https://nzjg.onlinelibrary.wiley.com/doi/10.1002/jgo2.70023 by CochraneItalia, Wiley Online Library on [10/03/2026]. See the Terms and Conditions (https://onlinelibrary.wiley.com/terms-and-conditions) on Wiley Online Library for rules of use; OA articles are governed by the applicable Creative Commons License

rock fragments. It has been chosen to adopt this classification to facilitate the comparison with the several petrographic literature datasets, rather than the Gazzi–Dickinson method (Gazzi 1966; Ingersoll et al. 1984), even if we are aware of the fact the this introduces a grain-size bias in the petrographic results. The Quartz, Feldspars, and Rock Fragments values of each sample used in this study are shown in Table S1. Moreover, the lithostratigraphic data from literature were reinterpreted in light of updated bio- and lithostratigraphic data of the study areas. In addition, new quantitative petrographic data regarding sandstone samples from Tasmania sequences are presented. Samples from Tasmania were collected from outcrops (Adventure Bay and Poatina sections) and from three drill cores (Thorp-1, Cygnet-2, and MPT-3) sampled in the core repository of the Mineral Resources Tasmania (Table S2). Point-counting was carried out, collecting 300 points per thin section; data are then plotted in ternary diagrams following McBride (1963). Based on the literature and sandstone analyzed composition, part of Thorp-1 and part of MPT-3 cores, Cygnet-2, and Adventure Bay samples from Tasmania are Late Permian (Cygnet Coal Measures and correlatives); part of Thorp-1 and part of MPT-3 cores, and Poatina are Early Triassic (Quartz Sandstones and correlatives).

Multidimensional scaling (MDS) analysis was performed on QFRf ternary diagram data to support the quantitative petrographic analyses, highlighting compositional similarities between samples from different sectors and time intervals (Vermeesch 2013; Vermeesch and Garzanti 2015). For each ternary diagram shown in Figure 3 the arithmetic mean has been calculated and used as input in the provenance R package from (Vermeesch et al. 2016). A classical MDS scaling was applied to map dissimilarities between samples as Euclidean distances in a bidimensional plot. Paleogeographic reconstructions have been taken from Merdith et al. (2021), visualized with GPlates software (Muller et al. 2018) and modified in vectorial format in Adobe Illustrator.

4 | Sandstone Composition and Stratigraphy

Petrographic data are shown in six time steps that reflect the main changes in the depositional basin evolution. Moreover, data are divided following their geographic distribution (Figures 1, 3), identifying five areas that correspond to different portions of the Transantarctic Basin: CTAM include data from the Beardmore Glacier area; SVL include data from the Dry Valleys to Convoy Range; PAM include data from the region between Mulock to David glaciers; NVL include data from the Eisenhower to the Lanterman ranges; and TAS include data from Tasmania. Quantitative petrographic data of the CTAM are from Barrett et al. (1986); data of SVL are from Korsch (1974), McPherson (1975), Walker (1980), Collinson et al. (1983), Zurli (2018), Cornamusini et al. (2023), and Zurli et al. (2024a); data of the PAM are from Bernet and Gaupp (2005) and Olivetti et al. 2026; petrography of NVL is from Collinson et al. (1986), Di Giulio et al. (1999), Cornamusini et al. (2017), Zurli (2018), and Bomfleur et al. (2021); and petrographic data of Tasmania are from Collinson et al. (1990) and this work. Representative microphotographs of the investigated sandstones are shown in Figures 4, 5.

4.1 | Devonian

Quantitative petrographic analyses on Taylor Group strata are limited in number and they do consider all the formations, which represent deposition in different sedimentary environments (Bradshaw 2013; Cox et al. 2012). In the CTAM, the Taylor Group, represented by the Alexandra Fm (Figure 2), is thin (max ca. 300 m; Barrett 1991); nevertheless, the strata are dominated by mature quartzose sandstones, with well-rounded and quartz-cemented grains (Barrett et al. 1986). Feldspars and lithic fragments are rare. In SVL, where the Taylor Group reaches its maximum thickness (ca. 1400 m; Barrett 1991), quantitative petrographic analyses were carried out in the youngest formations (Altar Mountain Fm, Arena Sandstone, Beacon Heights Orthoquartzite, and Aztec Siltstone; Figure 2) by Korsch (1974) and McPherson (1975). The analyzed sandstones are strongly dominated by quartz, except for the Altar Mountain Fm sandstones that are subarkoses (Figure 3). Cemented, well-rounded, monocrystalline, with mainly normal extinction quartz, is the main mineralogical constituent of the Taylor Group sandstones, followed by alkali feldspars and minorly plagioclase; metamorphic lithic grains are rare, as well as heavy minerals (Figures 4, 6; Korsch 1974). In the Altar Mountain Fm, alkali feldspars are more common, and quartz grains are more angular (Korsch 1974). U–Pb detrital zircons on the uppermost formation in SVL (Aztec Siltstone) show an age dominated by the Mesoproterozoic and Late Neoproterozoic–Cambrian grains (Paulsen et al. 2017a). Deposition is not recorded during the Devonian neither in NVL nor Tasmania, which are both affected by igneous activity (Glen and Cooper 2021).

4.2 | Late Carboniferous–Early Permian

The sedimentation started in the latest Carboniferous-earliest Permian, where glacigenic strata filled the morphological lows related to the Maya Erosion Surface with a high thickness variability from 0 to 400 m in Antarctica and up to >500 m in Tasmania (Barrett 1991; Isbell et al. 1997; Reid et al. 2014). The glacigenic strata represent deposition at the end of the P1 event of the LPIA (Fielding et al. 2008; Isbell et al. 2012, 2008). These rocks were deposited in a wide range of sedimentary environments: subaqueous, likely glacio-marine in CTAM and possibly in SVL (Barrett et al. 1986; Isbell 2010; Isbell et al. 2008; Ives and Isbell 2021; Koch and Isbell 2013; 2022b), glacio-continental and glacio-lacustrine in NVL (Laird and Bradshaw 1981; Collinson et al. 1986; Cornamusini et al. 2017; 2022b), and glacio-marine in Tasmania (Henry et al. 2012; Reid et al. 2014; Ives et al. 2022; Zurli et al. 2022a). Quantitative petrographic analyses were carried out both on the diamictite matrix and sandstone levels interbedded within diamictites (Barrett et al. 1986; Cornamusini et al. 2017; Zurli 2018). The ternary diagrams and the MDS show that CTAM and SVL have a similar and homogeneous composition, dominated by quartz, with subordinate feldspars and rock fragments (Figures 3, 5). A feature of the tillite composition is the occurrence of polycyclic well-rounded quartz mixed with first-cycle angular quartz (Figure 4; Barrett et al. 1986; 2022b). On the contrary, in NVL, the composition differs from SVL and CTAM, with more common feldspars and rock fragments (Figure 3) that are mainly metamorphic and intrusive

11758791, 2026, 1, Downloaded from https://nzjg.onlinelibrary.wiley.com/doi/10.1002/jgg2.70023 by CochraneItalia, Wiley Online Library on [10/03/2026]. See the Terms and Conditions (https://onlinelibrary.wiley.com/terms-and-conditions) on Wiley Online Library for rules of use; OA articles are governed by the applicable Creative Commons License

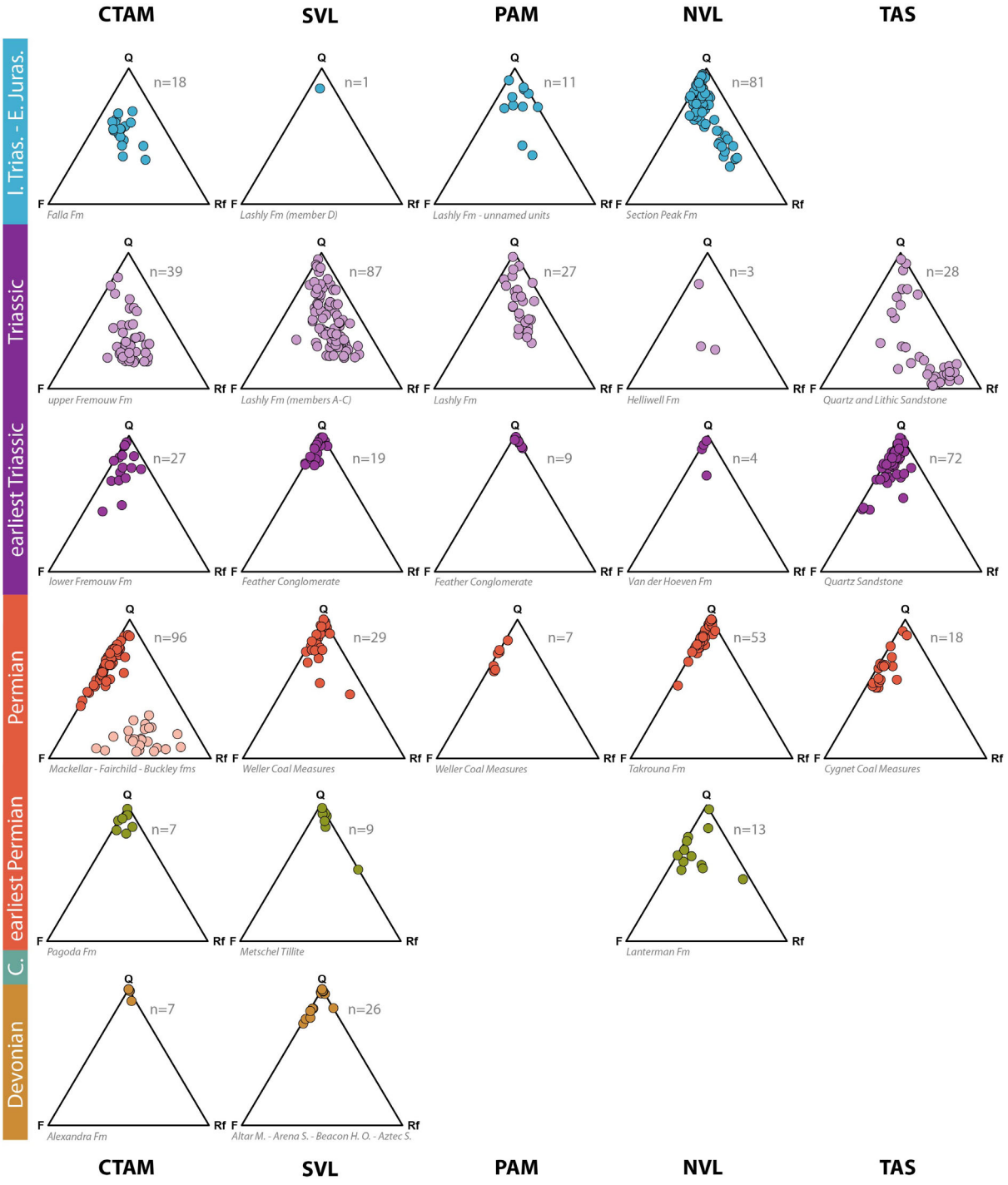

FIGURE 3 | Ternary diagrams of the sandstone composition following McBride (1963). The number of samples and the name of the formations are shown. For the Central Transantarctic Mountains, the dark orange circles represent the lower part of the Buckley Formation, the light orange ones the middle and upper part of the Buckley Formation. Q: quartz (monocrystalline and polycrystalline); F: feldspars (monocrystalline); Rf: rock fragments (quartz and feldspars in lithics and fine-grained volcanic-sedimentary-metamorphic lithic fragments). CTAM: Central Transantarctic Mountains, SVL: southern Victoria Land, PAM: Prince Albert Mountains, NVL: northern Victoria Land, TAS: Tasmania.

(Cornamusini et al. 2017; 2022b). This difference is due to the diversified composition of the bedrock of the clastic basin with the lower Permian tillite as the first deposit; indeed, the NVL lacks the Taylor Group strata, occurring in CTAM and SVL, which also represent a source for glacigenic strata, as pointed out by petrographic and geochronological studies (Barrett et al. 1986; 2022b). Those differences are also reflected in the composition of the gravel-size clasts of the tillite (Zurli et al. 2024b). Even if quantitative petrographic data are not available from Tasmanian diamictite, data from the clast composition and detrital zircon U–Pb geochronology, reveal differences with those of the Victoria Land and CTAM (Ives et al. 2022; Ives and Isbell 2021; Zurli et al. 2022a), supporting the great influence of the local basement on the sediment composition.

11758791, 2026, 1, Downloaded from https://nzjg.onlinelibrary.wiley.com/doi/10.1002/jgo2.70023 by CochraneItalia, Wiley Online Library on [10/03/2026]. See the Terms and Conditions (https://onlinelibrary.wiley.com/terms-and-conditions) on Wiley Online Library for rules of use; OA articles are governed by the applicable Creative Commons License

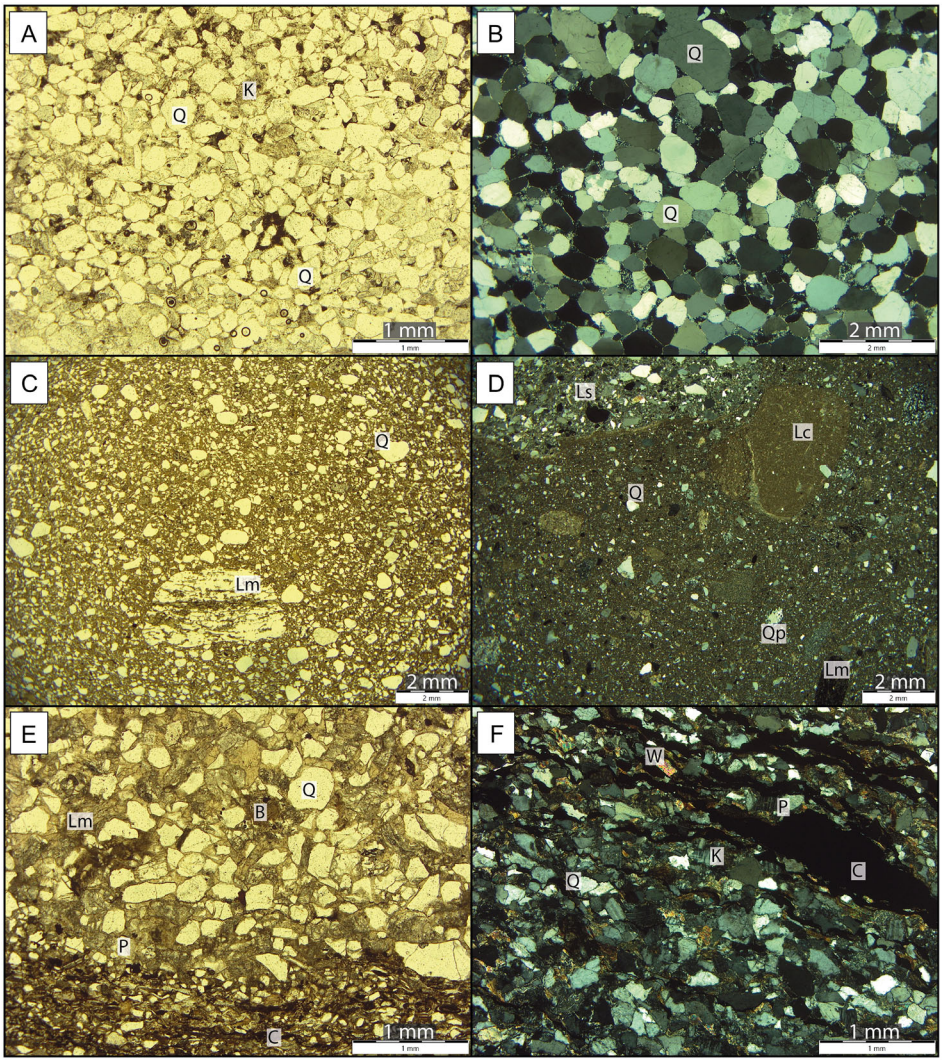

FIGURE 4 | Parallel and crossed polarized light microphotographs of Beacon and Parmeener supergroups sandstones. (A,B) Devonian Beacon Heights Orthoquartzite from SVL; (C) upper Carboniferous-lower Permian Metschel Tillite from SVL; (D) upper Carboniferous-lower Permian Wynyard Tillite from Tasmania; (E) Permian Weller Coal Measures from SVL; and (F) Permian Cygnet Coal Measures from Tasmania. B: biotite; C: carbonaceous material; K: alkali feldspar; Lc: carbonate lithic fragment; Lm: metamorphic lithic fragment; Ls: clastic sedimentary lithic fragment; P: plagioclase; Q: monocrystalline quartz; Qp: polycrystalline quartz; W: white mica.

4.3 | Permian

Permian records the transition between icehouse to greenhouse conditions, and in the Transantarctic Basin a moderate- to low-sinuosity fluvial systems in vegetated floodplains, allowing the deposition of thick coal intervals (Collinson et al. 1986; Barrett 1991; Isbell and Cúneo 1996; Schöner and John 2014; Cornamusini et al. 2017, 2023; Gulbranson et al. 2020). The post-glacial deposition in CTAM started with a flooding surface that rapidly evolved into a deltaic and fluvial system that characterized also SVL, PAM, and NVL (Isbell and Cúneo 1996; Isbell et al. 1997, 2008). On the contrary, the Permian deposition in Tasmania occurred in a shallow marine environment (Reid et al. 2014), with episodes of ice-distal influence and only in the late Permian a fluvial system developed (Fielding et al. 2010; Reid et al. 2014).The direction of paleocurrent indicators, mainly southward in CTAM and northward in Victoria Land (Barrett et al. 1986; Collinson et al. 1994, 1986; Schöner and John 2014; Cornamusini et al. 2023; Isbell and Cúneo 1996), led to the hypothesis that deposition occurred in separate basins divided by a morphological high (i.e., the Ross High; Collinson et al. 1994) separating the Transantarctic Basin in CTAM and the Victoria sub-basin in SVL. Based on low-temperature thermochronology on apatite and zircon grains, Olivetti et al. 2026 recorded the uplift of the PAM area in the Late Paleozoic, supporting the hypothesis of a morphological high (i.e., Prince Albert High) further dividing SVL and NVL sub-basins. In CTAM, the Mackellar, Fairchild, and the lower part of the Buckley sandstones are arkose to subarkose in composition (Barrett et al. 1986). However, from the middle part of the Buckley Formation, an abrupt compositional change has been recorded, marked by the appearance of lithic fragments constituting more than 50% in the QFL composition (Figure 3, 5). These rock fragments are mainly volcanic in origin with both microcrystalline and flow texture and porphyritic lava fragments, while glass and shard are less common (Barrett et al. 1986; Elliot et al. 2015, 2017a). Zircon U–Pb analyses yielded the youngest peaks between 260–250 Ma, revealing that volcanic detritus derived from the volcanic arc related to the Gondwanide Orogeny developed during the Permian, which is

11758791, 2026, 1, Downloaded from https://nsrz.onlinelibrary.wiley.com/doi/10.1002/jgo2.70023 by CochraneItalia, Wiley Online Library on [10/03/2026]. See the Terms and Conditions (https://onlinelibrary.wiley.com/terms-and-conditions) on Wiley Online Library for rules of use; OA articles are governed by the applicable Creative Commons License

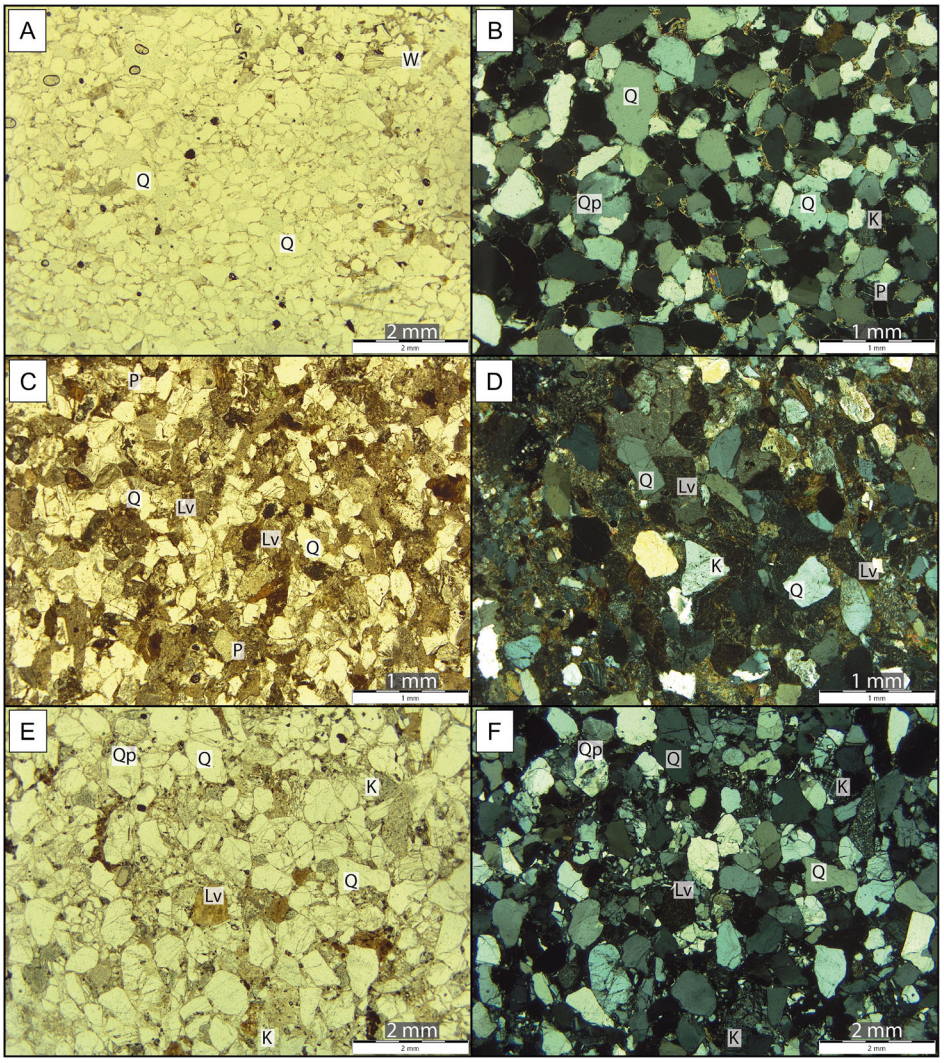

FIGURE 5 | Parallel and crossed polarized light microphotographs of Beacon and Parmeener supergroups sandstones. (A) Lowermost Triassic Feather Conglomerate from PAM; (B) lowermost Triassic Feather Conglomerate from SVL; (C) Triassic Lashly Fm from SVL; (D) Triassic Lashly Fm from PAM; and (E,F) upper Triassic-Lower Jurassic Section Peak Fm from NVL. K: alkali feldspar; Lv: volcanic lithic fragment; P: plagioclase; Q: monocrystalline quartz; Qp: polycrystalline quartz; W: white mica.

absent in the lower formations (Elliot and Fanning 2008; Elliot et al. 2015; Elliot et al. 2017a; Paulsen et al. 2017b). However, quantitative petrography shows a strong similarity between sandstones of the Weller Coal Measures (SVL) and of the Takrouna Formation (NVL), analogously to the PAM and to Tasmania. On the contrary, CTAM show two petrographic populations (Figure 3): the first, characterizing the lower part of the Buckley Fm, is similar to the other areas; the second, that is in the upper part of the Buckley Fm, is richer in rock fragments (Figure 6). As for the former, sandstones are arkoses and subarkoses to quartzarenites, mainly made up of mono- and polycrystalline quartz, followed by alkali feldspars and plagioclase, while metamorphic lithic fragments are scarce (Figure 4) and micas and heavy minerals are common (Collinson et al. 1986; John 2014; Cornamusini et al. 2017, 2023; Bomfleur et al. 2021; Zurli et al. 2024a). Detrital zircon U–Pb and mineral chemistry analyses also support provenance from the dismantling of the Ross Orogeny and minorly the East Antarctic Craton (Collinson et al. 1994, 1983, 1986; Lisker et al. 2006; Goodge and Fanning 2010; John 2014; Paulsen et al. 2017b; Zurli et al. 2024a). The PAM area outcrops are scattered due to ice cover and the large Ferrar Group rocks' emplacement and they show reduced thickness. The Permian strata occur at Ford Peak (Olivetti et al. 2026) and Beta Peak, where the Permian macroflora occurs (Capponi et al. 1999). Here, the Permian strata show petrographic features similar to the Weller Coal Measures (Figure 3). The Cygnet Coal Measures in Tasmania is constituted mainly by arkoses and subordinate subarkoses (Forsyth 1989), with a similar composition to the Transantarctic Basin sandstones (Figure 3), even if with a mean less abundance of quartz grains. Analyzed samples are fine to medium grained with subangular to subrounded clasts; matrix and pseudomatrix are common and poikilotopic calcite cement sometimes occurs. Grains are mainly made up of monocrystalline quartz with a minor amount of polycrystalline quartz, alkali feldspars, and plagioclase; feldspars are usually replaced by sericite and clay mineral aggregates. Lithic fragments are rare and usually made by fine-grained metamorphic and sedimentary rocks (Figure 6). Detrital white mica and biotite are common, as well as garnet crystals.

11758791, 2026, 1, Downloaded from https://nsrz.onlinelibrary.wiley.com/doi/10.1002/jgo2.70023 by CochraneItalia, Wiley Online Library on [10/03/2026]. See the Terms and Conditions (https://onlinelibrary.wiley.com/terms-and-conditions) on Wiley Online Library for rules of use; OA articles are governed by the applicable Creative Commons License

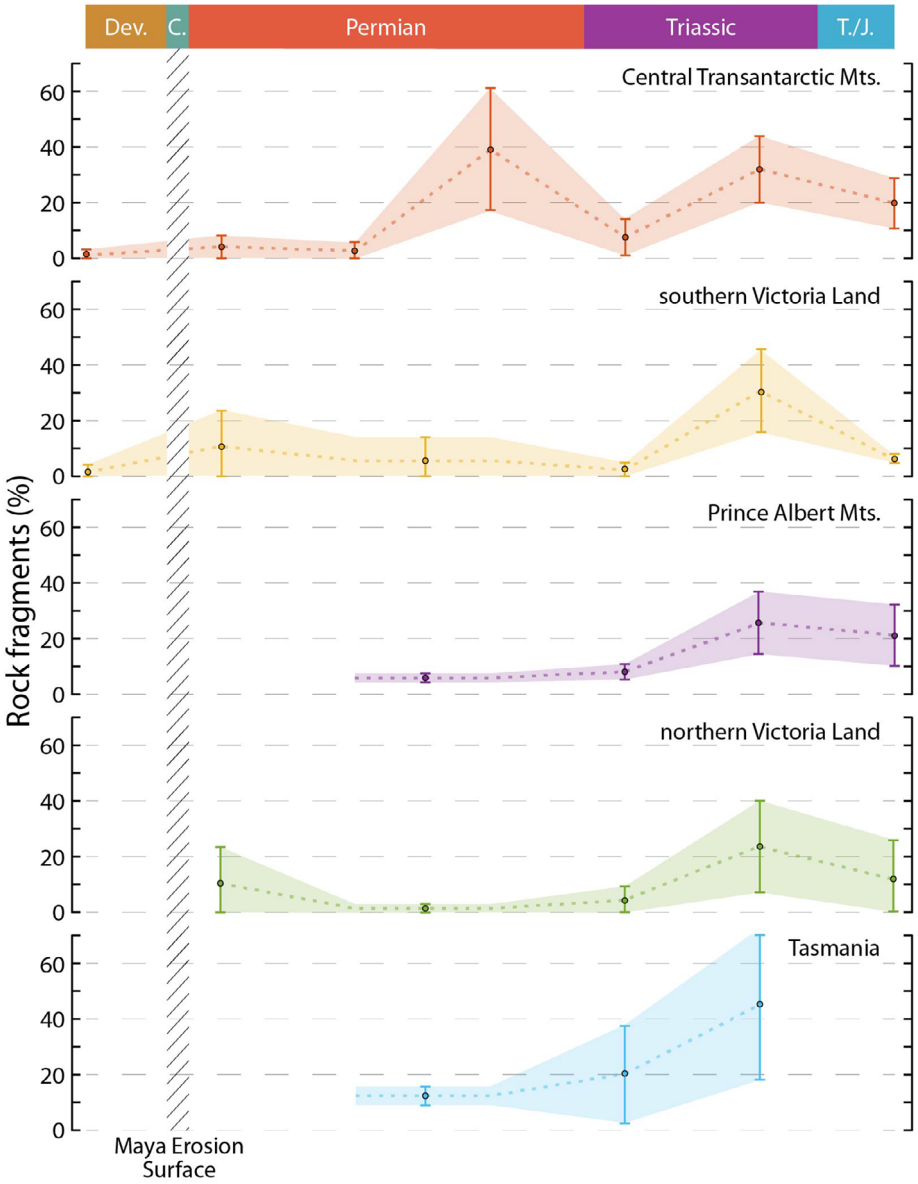

FIGURE 6 | Diagrams showing the spatial and temporal distribution of mean value of rock fragments. Light colored areas represent the standard deviation.

4.4 | Earliest Triassic

In the CTAM, the lower Freemouw Formation are subarkoses to quartzarenites, where quartz is the main mineralogical constituent, followed by alkali feldspars and plagioclase, while lithic fragments are less abundant (Figure 3). The latter are fine grained sedimentary and metamorphic rocks and volcanic ones, likely, at least partially, reworked from the underlying Buckley Formation (Barrett et al. 1986), as confirmed by U–Pb geochronological analyses that show mainly Ross Orogen ages and very rare Permian–Triassic zircon grains (Elliot and Fanning 2008). In SVL, the earliest Triassic deposition occurred in a braided fluvial system (Barrett and Fitzgerald 1985; Cornamusini et al. 2023) and the Feather Conglomerate is mainly made up of quartzarenites to subarkoses (Figures 3, 5), showing a decrease in feldspar content compared with the underlying Weller Coal Measures (Korsch 1974; Walker 1980; Collinson et al. 1983; Cornamusini et al. 2023; Zurli et al. 2024a). Detrital zircon content and mineral chemistry (Zurli et al. 2024a) support the hypothesis of a provenance from mainly Granite Harbor Intrusive Complex (Barrett and Fitzgerald 1985) or reworked deposits. In the PAM, the correlatives of the Feather Conglomerate strata are mainly quartzarenites and lie directly on the basement or above arkose strata with Permian Glossopteris flora (Olivetti et al. 2026). In NVL, the earliest Triassic units have been recently revealed for the lower Rennick Glacier region and defined as Van der Hoeven Fm (Bomfleur et al. 2021); it is dominated by quartzarenite beds with compositional features resembling those of the Feather Conglomerate in SVL (Bomfleur et al. 2021). In Tasmania, the Quartz Sandstone Fm represents the earliest Triassic deposit (Reid et al. 2014; Calver et al. 2023) and its composition is mainly quartzarenite to subarkose (Figure 3; this study; Clarke et al. 1989; Collinson et al. 1990). The main constituent is monocrystalline quartz, with minor feldspars, alkali feldspar more common than plagioclase, and lithic fragments mainly made by metasedimentary rocks (Clarke et al. 1989; Collinson et al. 1990).

11758791, 2026, 1, Downloaded from https://nsrz.onlinelibrary.wiley.com/doi/10.1002/jgo2.70023 by CochraneItalia, Wiley Online Library on [10/03/2026]. See the Terms and Conditions (https://onlinelibrary.wiley.com/terms-and-conditions) on Wiley Online Library for rules of use; OA articles are governed by the applicable Creative Commons License

4.5 | Early-Middle Triassic

In CTAM sandstones of the middle and upper part of the Fremouw Fm (Early to Middle Triassic) are characterized by subangular grains, dominated by volcanic lithic fragments, and minor quartz and feldspars, with plagioclase more common than alkali feldspar (Figure 3). Volcanic lithic fragments are mafic to intermediate in composition, with fine grained and slightly porphyritic, sometimes trachytic, texture (Barrett et al. 1986; Elliot et al. 2017a). Detrital zircons show that the main population is Triassic in age and the weighted mean age decreases upward (Paulsen et al. 2017b; Elliot et al. 2017a; Elliot et al. 2019). In SVL, the Lashly Fm, subdivided in several members, records an abrupt compositional change with respect to older strata (Figure 6). Indeed, excepting the lowermost part of Member A (Early Triassic), the sandstones are dominated by volcanic detritus, followed by quartz and feldspars, with abundant plagioclase grains (Figure 3, 5). Volcanic grains are fine grained, sometimes with trachytic texture, and variable in composition between felsic to mafic (Korsch 1974; Elliot and Grimes 2011; Cornamusini et al. 2023; Zurli et al. 2024a). This compositional change is also recorded by U–Pb zircon geochronology, showing that volcanic detritus is sourced by the Triassic arc developing in the paleo-Pacific margin of Gondwana (Zurli et al. 2024a). In PAM, sandstone outcrops, mainly made by fine-grained volcanic grains, quartz, and plagioclase, show petrographic features that make possible the correlation with the Lashly Fm that crops out southward (Figure 5; Olivetti et al. 2026). Capponi et al. (2024) indicate a palynostratigraphic assemblage referrable to the Middle Triassic, corresponding to the Lashly Fm depositional age; palynostratigraphic data from underlying strata show late Early Triassic age (Corti et al. 2026, under review—this volume), supporting the interpretation of these units. In NVL, sandstone outcrops corresponding to the Lashly Fm (Member A to C) and Fremouw Fm occur in the lower Rennick Glacier, where the Helliwell Fm crops out (Bomfleur et al. 2021). Despite the small number of samples, the composition of the sandstones of the Helliwell Fm strongly resembles the Lashly Fm and it is dominated by volcanic grains with a minor amount of quartz and feldspars (Bomfleur et al. 2021). By contrast, the sandstones of the Tasman succession show a different compositional distribution, with a population richer in quartz grains that characterizes the lower part of the Quartz and Lithic Sandstone Fm, and another population richer in lithic volcanic clasts (Figure 3). Syn-sedimentary volcanic activity has been evidenced by the occurrence of ash beds within the succession, dated to the Late Triassic (Carnian-Norian; Calver et al. 2021). Felsic to intermediate volcanic and hypoabyssal grains are the main constituent of the sandstones, followed by quartz and feldspars, that are mainly plagioclase; metamorphic lithic grains are also common (Figure 3; this study, Clarke et al. 1989; Collinson et al. 1990).

4.6 | Late Triassic–Jurassic

In the CTAM, the expression of the Late Triassic sedimentation is the Falla Formation (Farabee et al. 1989). The Falla Fm sandstones are quartzo-feldspatic in composition, with the occurrence of volcanic lithic grains with trachytic texture and sedimentary ones (Barrett et al. 1986; Elliot et al. 2017a); zircon U–Pb geochronological data point to a latest Triassic (Norian) age (Elliot et al. 2017a). Above the Falla Fm, the Hanson Fm (Elliot 1996) disconformably occurs. This last consists of quartzose sandstones interbedded with dominant tuffs in the lower member, tuffs interlayered with volcaniclastic sandstones in the middle member, and tuffs in the upper member (Elliot et al. 2017b); geochronological analyses show the Early Jurassic age for the Hanson Fm (Elliot et al. 2017b). In SVL, Lashly Fm deposition continues until the Late Triassic, marking a further lithological and compositional change, from lithic arenites in the members A to C, to quartz-dominated sandstones, in the Member D (Collinson et al. 1983 Elliot and Grimes 2011). Above the Member D of the Lashly Fm, the deposition of quartz dominated sandstones is alternated with silicic tuff layers (unnamed units), ascribed to the Early Jurassic (Elliot and Grimes 2011). The sandstone beds' main composition resembles those of the upper Lashly Fm, even if the grain size is smaller, micas and heavy minerals are more common, and pumice grains occur; tuffaceous strata show variable content of quartz, feldspar, and silicic glass shard (Elliot and Grimes 2011). In the PAM area, carbonaceous mudstone interlayered with sandstones and tuffs yield Early Jurassic palynomorphs (Unverfärth et al. 2020; Corti et al. 2026, under review). Sandstone composition shows a wide variability from quartz-dominated samples (subarkose to sublitharenite) to subordinate lithic fragment-dominated ones; the latter present abundant volcanic and glass grains (Bernet and Gaupp 2005; Olivetti et al. 2026). In NVL, the correlative of Member D of the Lashly Fm is represented by the lower Section Peak Fm, which is Late Triassic in age (Bomfleur et al. 2011, 2014), and lies directly onto the crystalline basement in the Deep Freeze Range (Schöner et al. 2011). The upper Section Peak Fm, disconformably overlying the lower Section Peak Fm or directly the crystalline basement, is Early Jurassic in age and correlative of the unnamed units in SVL and PAM (Norris 1965; Collinson et al. 1986; Pertusati et al. 2006; Schoner et al. 2011; Bomfleur et al. 2011, 2014, 2021). The Early Jurassic sandstone layers of the Shafer Peak Fm are instead interlayered with silicic tuff strata (Schoner et al. 2011). The composition of the sandstones varies from quartz-feldspars dominated to felsic to mafic volcanic lithic grains dominated (Figures 3, 5; Collinson et al. 1986; Elsner 2010; Schoner et al. 2011). Di Giulio et al. (1999) show the occurrence of mafic volcanic grains in correspondence with volcanic layers, interpreted as basalt lava flows, suggesting the contemporaneous deposition of siliciclastic strata and volcanic activity. Geochronological U–Pb analyses on the upper Section Peak Fm reveal the occurrence of Early Jurassic zircons, together with Triassic, Early Paleozoic-Late Neoproterozoic, and Mesoproterozoic ages (Goodge and Fanning 2010; Elsner et al. 2013), supporting the coeval volcanic and sedimentary activity. In the Tasman Basin, there is no evidence for the latest Triassic to Early Jurassic deposits (Reid et al. 2014).

5 | Multidimensional Scaling

Differences and similarities among each time–space intervals have been visualized with the MDS map (Figure 7). Data in the bottom left of the map have a composition dominated by quartz and feldspars, reflecting a source from the basement, while data on the top right of the map have a composition dominated by volcanic lithic fragments, reflecting a source from volcanic rocks. The map of Figure 7 shows that SVL and CTAM are

11758791, 2026, 1, Downloaded from https://nzjg.onlinelibrary.wiley.com/doi/10.1002/jgo2.70023 by CochraneItalia, Wiley Online Library on [10/03/2026]. See the Terms and Conditions (https://onlinelibrary.wiley.com/terms-and-conditions) on Wiley Online Library for rules of use; OA articles are governed by the applicable Creative Commons License

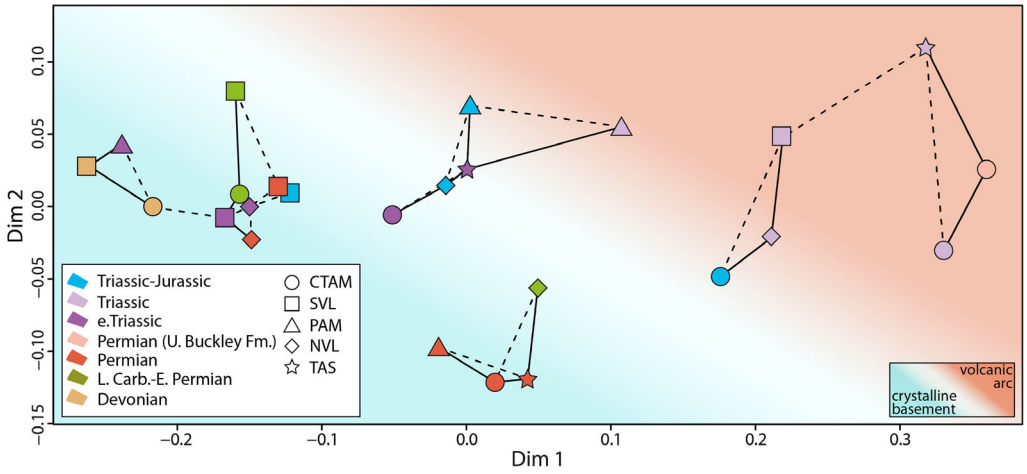

FIGURE 7 | Multidimensional scaling map of the petrographic population for each studied area and timestep. CTAM: Central Transantarctic Mountains, SVL: southern Victoria Land, PAM: Prince Albert Mountains, NVL: northern Victoria Land, TAS: Tasmania.

strongly similar in the Devonian; sandstones are mainly made by quartz, and the points occupy the left part of the map. The Late Carboniferous–early Permian glaciogenic strata show wide dispersion on the map, supporting the strong influence of the local bedrock in their composition. Indeed, CTAM and SVL, where the Devonian Taylor Group is present, values are close, while in NVL, where glaciers flowed onto the crystalline basement, the point is not connected with the coeval ones. About the Permian, SVL and NVL points are close but not directly connected; CTAM, PAM, and Tasmania show quite a similar evolution. An additional point of data is considered for the late Permian in the CTAM to highlight the compositional heterogeneity arising from quartz-rich sandstone reflecting a low-land arrangement toward the volcanic arc source (Figures 3, 5). In the earliest Triassic SVL, PAM, and NVL show compositional affinity; conversely, CTAM and Tasmania are shifted toward a light occurrence in volcanic rocks, reflecting the higher dispersion in point data (Figure 3). In the Triassic sandstone compositions, all studied sectors shift to the upper right half of the MDS plot, indicating a transition to volcanic arc as the main source. Across the latest Triassic and Early Jurassic, sandstone composition is highly variable (Figure 3) and the mean values used for the MDS plot show that points plot in an intermediate portion of the map.

6 | Discussion

6.1 | Devonian

The sedimentation of the Devonian Taylor Group occurred in SVL within an epi-cratonic basin (Woolfe and Barrett 1995), sourced by the dismantling of the East Antarctic craton and the crystalline rocks formed during the Ross Orogeny, similarly to the portion of the basin for the CTAM (Barrett 1991; Paulsen et al. 2017a). On the contrary, PAM, NVL, and Tasmania did not recorded sedimentation in the Devonian (unless the complete erosion of these strata). Deformation and magmatism affected Tasmania (Berry and Bull 2012), whereas NVL was emplaced by the Admiralty Intrusives (Henjes-Kunst and Kreuzer 2003). The inferred retro-arc foredeep is bounded by a forebulge, which was considered subaerial and hindered the bypass of arc-derived sediments toward Victoria Land. On top of the forebulge, an erosional surface is expected (Horton 2022) and the sediment bypass from the foredeep to the back-bulge (epi-cratonic basin) is minimal. The underfilled condition of the foredeep may depend on the competing action of flexural uplift over dynamic subsidence (e.g., Catuneanu 2004). Following this evidence, such areas as PAM and overall NVL and TAS, represented morphological highs (Figure 8), respectively marginal and external to the basin, lacking any sedimentation, where basement erosion occurred. High-temperature thermochronological data indicate high erosion rates along the Queen Maud and Ross highs, which fits with the Devonian nondeposition phase in the southern TAM and in the Ross Hight regions (Paulsen et al. 2025).

6.2 | Late Carboniferous–Earliest Permian

The Late Carboniferous-earliest Permian is characterized by widespread ice covers that led to the deposition of thick glacigenic successions in the southern Gondwana. Glacial flows and glacigenic deposition were likely driven by pre-existing tectonic structures, forming irregular and erosional bottom surfaces

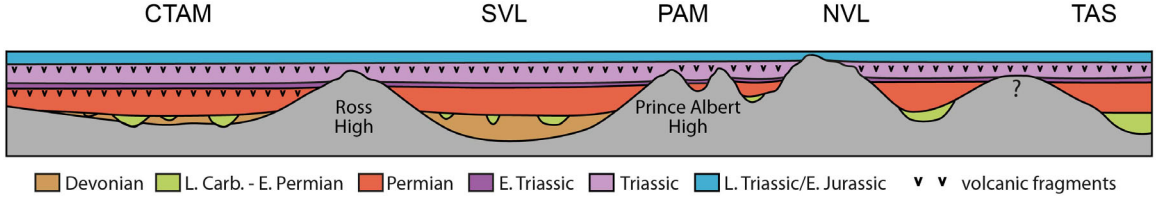

FIGURE 8 | Exemplificative schematic stratigraphic section along the Transantarctic Basin. The image is not in scale and the transect is idealized. CTAM: Central Transantarctic Mountains, SVL: southern Victoria Land, PAM: Prince Albert Mountains, NVL: northern Victoria Land, TAS: Tasmania.

11758791, 2026, 1, Downloaded from https://nsrz.onlinelibrary.wiley.com/doi/10.1002/jgo2.70023 by CochraneItalia, Wiley Online Library on [10/03/2026]. See the Terms and Conditions (https://onlinelibrary.wiley.com/terms-and-conditions) on Wiley Online Library for rules of use; OA articles are governed by the applicable Creative Commons License

(Figure 8; Isbell et al. 1997). The ice flow indicators show that ice tongues departing from the main ice caps flowed transversally in a main elongated basinal depression, parallel to the present-day TAM direction, from both basin flanks (Isbell 2010). Petrographic and geochronological studies do not indicate syn-depositional volcanic activity (Elliot et al. 2015; Cornamusini et al. 2017; Craddock et al. 2019; Zurli et al. 2022b, 2024b). Paleo-ice flow directions indicate an articulated paleo-morphology in Tasmania (Hand 1993) with glaciers flowing in a marine environment and sediment sourced from the local basement (Fielding et al. 2010; Henry et al. 2012; Ives, Isbell & Licht 2022; Zurli et al. 2022b; Ives et al. 2023).

6.3 | Permian

At the end of the glacial phase and during the Permian, the alluvial systems were widespread throughout southern Gondwana (Figure 8), as such as all along the southern and northern Gondwana supercontinent, generating quartz-rich sandstone suites (e.g. Critelli et al. 2022; Criniti et al. 2024). The onset of neovolcanic activity dilutes the quartzose and quartzolithic sandstone suites testified by feldspatholithic volcaniclastic sandstone suites on both southern (present work) and northern (Criniti et al. 2023) continental margins of Gondwana. The respective Permian sandstones recorded the beginning of the volcanic activity related to the Gondwanide Orogeny that developed due to the subduction of the paleo-Pacific oceanic plate under the southern Gondwana margin. The Permian magmatic rocks currently crop out (Figure 9) in eastern Marie Byrd Land and Antarctic Peninsula (Nelson and Cottle 2018; Jordan et al. 2020 and reference therein) and New Zealand (Campbell et al. 2020). In the CTAM, the basin started to receive volcanic detritus (Figure 6), eroded from the volcaniclastic wedge in front of the volcanic arc, in the upper part of the Buckley Fm (Elliot et al. 2015), but it is substantially absent for the sequences of the Victoria Land. This hypothesis, shown in Figure 9, is consistent with the occurrence of a morphological high, the Ross High, separating the Victoria Land sub-basin from the main Transantarctic Basin (Collinson et al. 1994), and supported by thermochronological data along the Queen Maud and Ross highs (Paulsen et al. 2025). Moreover, thermochronology in the PAM indicates that this sector of the forebulge, the Prince Albert High, experienced exhumation until the Triassic (Olivetti et al. 2026), representing the northern edge of the SVL sub-basin. Indeed, in SVL and NVL the fluvial deposits did not record the volcaniclastic input (Figure 6), supporting the hypothesis that Victoria Land sub-basins were in a backbulge position. Differently, PAM and NVL areas were peripheral to the basin with high-relief and very irregular morphology, subjected to local sedimentation within small and poorly subsident fluvial basins (Figures 8, 9). In the Tasmania Basin, the Permian deposition passes from marine to continental in the late Permian (Clarke 1989). The basin was characterized by morphological highs with no deposition (Clarke 1989) that could represent highs of the forebulge system; indeed, the composition of the upper Permian sandstones is quartz-feldspatic dominated and volcanic input was not recorded (Figure 3). In the opposite position of the Transantarctic Basin, in the Ellsworth Mountains sector, the Permian Polarstar Fm, deposited in the Transantarctic Basin (Collinson et al. 1994), recorded coeval volcanic input, including tuff layers, since its base (Elliot et al. 2016; Craddock, et al.

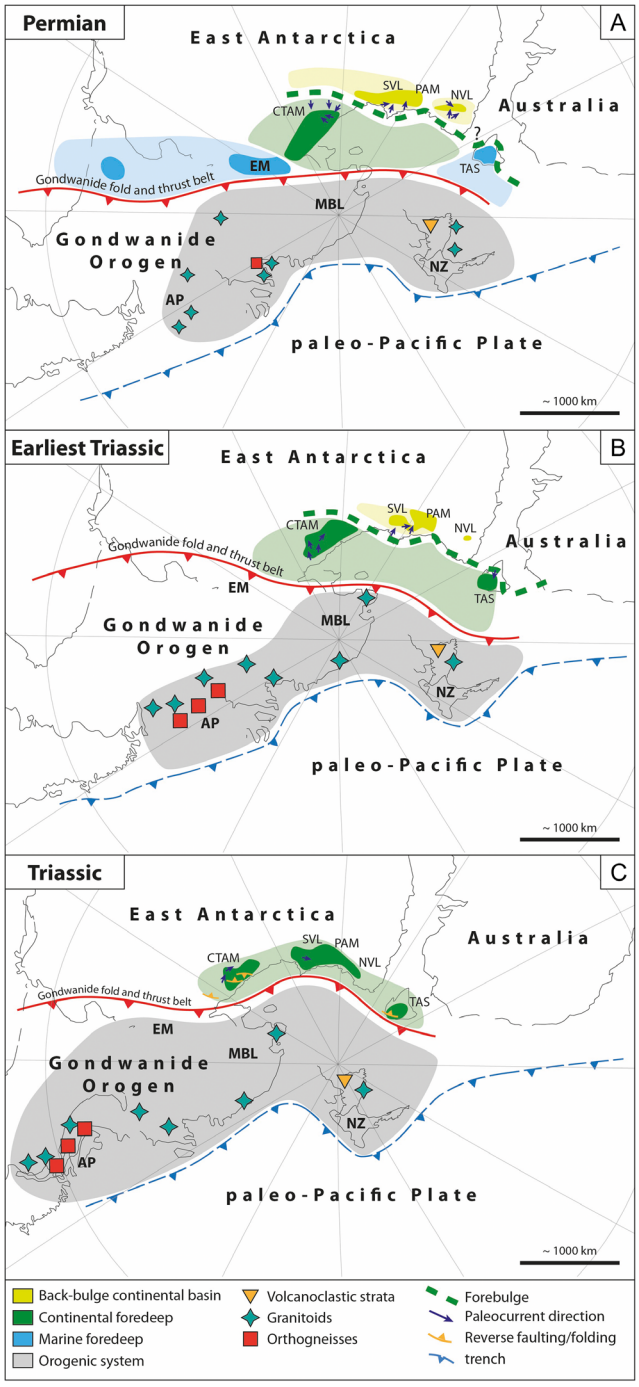

FIGURE 9 | Schematic paleogeographic reconstructions of the southern Gondwana margin evolution in three timesteps: (A) Permian, (B) earliest Triassic, and (C) Triassic. Plate assemblages are from Merdith et al. (2021) and visualized with GPlates software (Müller et al. 2018). Position of the granitoids and orthogneisses are modified from Elliot (2013) and Elliot et al. (2019). Position of the fold and thrust belt and forebulge are modified from Collinson et al. (1994) and (Zurli et al. 2024a). Paleocurrent directions are from Barrett (1991), Collinson et al. (1994), (Zurli et al. 2024a). Faults and folds are from Berry and Banks (1985) and Elliot (2024). Dark colors represent cropping out areas while shaded colors represent areas where outcrops are inferred. AP: Antarctic Peninsula, CTAM: Central Transantarctic Mountains, MBL: Marie Byrd Land, NVL: northern Victoria Land, NZ: New Zealand, PAM: Prince Albert Mountains, SVL: southern Victoria Land, TAS: Tasmania.

11758791, 2026, 1, Downloaded from https://nzjg.onlinelibrary.wiley.com/doi/10.1002/jgo2.70023 by CochraneItalia, Wiley Online Library on [10/03/2026]. See the Terms and Conditions (https://onlinelibrary.wiley.com/terms-and-conditions) on Wiley Online Library for rules of use; OA articles are governed by the applicable Creative Commons License

2017a), supporting that this portion was part of the foredeep since the early Permian. In summary, during the Permian the basin in the southern Gondwana margin shows different geodynamic settings, characterized by a westward migration of the foredeep: the Ellsworth Mountains and the CTAM were part of the foredeep since the early Permian, while the Victoria Land sub-basins and the Tasmania Basin were in a backbulge setting (Figure 9).

6.4 | Earliest Triassic

The Permian–Triassic boundary marks a shift in sandstone composition all along the southern Gondwana margin, with the rapid decrease of volcanic grain input in CTAM and of feldspars for all the other areas, accompanied by a relative enrichment in quartz grains (Figures 3, 6). Detrital zircons also show a strong decrease of the Permian-Triassic population in CTAM (Elliot and Fanning 2008) and its absence in SVL (Zurli et al. 2024a). It could be speculated that the development of a morpho-structural high in the foreland basin impeded the transport of the volcanic detritus, while the sediment of the basin was sourced mainly from the dismantling of the high, which was composed of basement rocks. The quartz-dominated composition and the common occurrence of rounded quartz grains point to the occurrence of polycyclic sediments. Indirect evidence of tectonic activity in the earliest Triassic is the change of the fluvial style in SVL (Collinson et al. 1994; Zurli et al. 2024a), which could change the source areas also in terms of increase in relief. Indeed, the earliest Triassic Feather Conglomerate marks a shift from a meandering/anastomosed system during the Permian to a braided system (Barrett & Fitzgerald 1985; Barrett 1991; Collinson et al. 1994; Cornamusini et al. 2023). Relief development may be the result of steepening of the thrust and fold belt foreslope and intrafore-land uplift (e.g., Olivetti et al. 2026). A possible explanation for the large scale of the deformation belt and the uplift in the foreland system, as proposed for the Andes (Bishop et al. 2018; Horton 2022; Horton et al. 2022), could be the flat-slab subduction of the paleo-Pacific plate under Gondwana lithosphere, which was also hypothesized in south Gondwana (Navarrete et al. 2019; Bastias et al. 2021; Olivetti et al. 2026).

6.5 | Early-Middle Triassic

After the quartz-dominated coarse sandstone deposition that characterized the earliest Triassic, the deposition along the entire southern Gondwana margin recorded a significant compositional change (Figure 6). Sandstones show everywhere a marked increase in lithic grain component, made up of mafic to felsic volcanic rocks and the Triassic population is dominant in the detrital zircons (Elliot et al. 2017a; Zurli et al. 2024a). The huge volcaniclastic input suggests that the morphological highs that characterized and subdivided the basin in the first phases, at least since the Permian to the earliest Triassic, no longer acted as significant barriers to the clastic drainage-feeding systems (Figure 8). The sediments were mostly eroded from the volcanic rock of the Gondwanide arc, but also from the intrusive and metamorphic rocks of the basement, albeit to a lesser extent. During the Triassic, the sandstone composition was uniform in the Transantarctic Basin (Figure 3), particularly for the CTAM and SVL. Differently, PAM and NVL recorded reduced sedimentation within smaller and fragmented basins, with deposition also directly on the basement rocks, due to the effects of differentiated uplift related to tectonic activity (Figure 8). The Ross High was buried by the sedimentary cover and no longer act as a significant morphological barrier; paleo-current indicators within the Triassic sequences (Figure 9) support this hypothesis, with the main direction from the CTAM toward Tasmania (Collinson et al. 1994). In this regard, in the Triassic, the Transantarctic Basin was part of the foredeep basin (Figure 9). In this depositional and stratigraphic framework, the absence of the Middle Triassic deposits for the southern part of NVL (i.e., Deep Freeze Range; Figure 8) is probably related to the structuration of morphological highs due to tectonics, determining a local alternance with depressions, causing an irregular stratigraphy, even if the alluvial systems were probably connected. Evidence of the involvement of some sectors of the foreland basin in the fold and thrust belt at the orogeny front is rare. The Ellsworth Mountains clearly show the effects of the tectonic deformation (Elliot et al. 2016, Craddock, et al. 2017a). However, compressive tectonic indicators occur in some sectors of the basin (Figure 9): Elliot (2024) reported reverse faulting in the southern and CTAM, at Nilsen Plateau and Queen Alexandra Range; Tasmania also shows evidence of reverse faulting under a stress field corresponding to shortening oriented normal to the inferred main deformation belt (Berry and Banks 1985). In a scenario with a more proximal deformation front, the foredeep, now overfilled due to the higher sediment discharge driven by topographic growth, is connected to all Transantarctic sub-basins, and local topographic highs were buried.

6.6 | Late Triassic–Jurassic

The Late Triassic is also characterized by a compositional change with the decrease of volcaniclastic input in the sedimentary deposits, with the relative increase in quartz grains (Figure 6). This change occurs all along the Transantarctic Basin (Falla Fm in CTAM, Member D of the Lashly Fm in SVL, lower Section Peak Fm in NVL) as result of four possible scenarios: the dismissal of erosion of the volcanic arc, the development of morpho-structural barriers due to thrusting that inhibited the volcanic detrital feeding within the basin, a tectonic inversion toward the development of retro-arc extension changing the detrital source systems, and the interruption of volcanic activity.

Since the Early Jurassic, clastic sedimentation was then alternated with silicic tuff deposition all along the Transantarctic Basin. Felsic volcanic products predated the mafic emplacement phase of the Ferrar Group (Elliot et al. 2017b), pointed toward the hypothesis of the development of a tensional phase, accompanied by magmatism, similarly to southern Patagonia (Navarrete et al. 2019; Bastias et al. 2021) and Ellsworth Mountains (Craddock, et al. 2017b), where the felsic volcanic rocks of the Chon Aike largely crop out.

7 | Conclusion

This work provides a source-to-sink model for the evolution of the Transantarctic and Tasmania basins through a synthesis and revision of literature and new quantitative petrographic data. Sandstone composition, compared with sedimentological, structural, and paleogeographic data, is used as a proxy to

11758791, 2026, 1, Downloaded from https://nzjg.onlinelibrary.wiley.com/doi/10.1002/jgo2.70023 by CochraneItalia, Wiley Online Library on [10/03/2026]. See the Terms and Conditions (https://onlinelibrary.wiley.com/terms-and-conditions) on Wiley Online Library for rules of use; OA articles are governed by the applicable Creative Commons License

understand the evolution of the basin through time. In the Devonian sedimentation was limited to SVL and CTAM and sandstone composition supports the epi-cratonic nature of the basin. During the Permian, the basin was divided into sub-basins separated by morpho structural highs that acted as barriers. Sandstone composition in the CTAM recorded the involvement of this portion of the basin in the foredeep of the Gondwanide orogen backside. On the contrary, sandstone compositions in Victoria Land and Tasmania show that these areas were not connected to the volcanic arc, and that they were likely deposited in the backbulge sector of the basins. In the earliest Triassic sandstones show a decrease of volcanic grains, likely occurred due to tectonic changes. Later, in the Early to Middle Triassic, sandstones show a generalized compositional change with an increase in volcanic lithic fragments that agree with the involvement of the volcanic arc source for all the sectors of the foredeep. The latest Triassic and Early Jurassic sandstone composition shows a decrease of volcanic grains, pointing to the formation of detrital feeding and drainage barriers between the basin and the volcanic arc. The last sedimentary activities were recorded during the onset of the Ferrar Large Igneous Province.

Acknowledgments

This work is supported by the Italian "Programma Nazionale di Ricerche in Antartide" (PNRA) [grant no. PNRA19_00120]. Field campaigns in Victoria Land and Tasmania have been supported by other PNRA projects led by the researcher team of the University of Siena. We are grateful to the Associate Editor of the special issue Dr Daeyeong Kim for his support during the publishing process, and to Prof Salvatore Critelli and two anonymous reviewers for their valuable comments on the manuscript. We wish to thank the National Museum of Antarctica – Siena Section (https://mna.it/sede-di-siena/) and its personnel for providing access to the collection of Antarctic rock samples. We would also like to thank Mineral Resources Tasmania (MRT) at the Mornington Core Library in Hobart which granted us the opportunity to study the Tasmania cores.

Open access publishing facilitated by Universita degli Studi di Siena, as part of the Wiley - CRUI-CARE agreement

Funding

This study was supported by the Ministero dell'Università e della Ricerca (PNRA19_00120).

Conflicts of Interest

The authors declare no conflicts of interest.

Data Availability Statement

The data that support the findings of this study are available from the corresponding author upon reasonable request.

References

Allen, P. A., and J. R. Allen. 2013. Basin Analysis: Principles and Application to Petroleum Play Assessment. 3rd. John Wiley & Sons.

Barrett, P. J. 1981. "History of the Ross Sea Region during the Deposition of the Beacon Supergroup 400 - 180 million Years Ago." *Journal of the Royal Society of New Zealand* 11, no. 4: 447–458. https://doi.org/10.1080/03036758.1981.10423334.

Barrett, P. J. 1991. "The Devonian to Jurassic Beacon Supergroup of the Transantarctic Mountains and Correlatives in Other Parts of Antarctica." In Geology Antarctic, ed. by R. J. Tingey, 120–152. Clarendon Press.

Barrett, P. J., and B. P. Kohn. 1975. "Changing Sediment Transport Directions from Devonian to Triassic in the Beacon Supergroup of South Victoria Land, Antarctica." In Gondwana Geology, ed. by K. S. W. Campbell, 15–35. A.N.U. Press.

Barrett, P. J., and P. G. Fitzgerald. 1985. "Deposition of the Lower Feather Conglomerate, a Permian Braided River Deposit in Southern Victoria Land, Antarctica, with Notes on the Regional Paleogeography." *Sedimentary Geology* 45: 189–208.

Barrett, P. J., and P. N. Webb. 1973. "Stratigraphic Sections of the Beacon Supergroup (Devonian and Older (?) to Jurassic) in South Victoria Land." In Publication of Geology Department Antarctic, 1–165. Victoria University of Wellington.

Barrett, P. J., B. P. Kohn, R. A. Askin, and J. G. McPherson. 1971. "Preliminary Report on Beacon Supergroup Studies between the Hatherton and Mackay Glaciers." *New Zealand Journal of Geology and Geophysics* 14, no. 3: 605–614. https://doi.org/10.1080/00288306.1971.10421951.

Barrett, P. J., D. H. Elliot, and J. F. Lindsay. 1986. "The Beacon Supergroup (Devonian-Triassic) and Ferrar Group (Jurrasic) in the Beardmore Glacier Area, Antarctica." In Antarctic Research Series, ed. by M. D. Turner and J. F. Splettstoesser. 339–428. https://doi.org/10.1029/AR036p0339.

Bastias, J., R. Spikings, T. Riley, et al. 2021. "A Revised Interpretation of the Chon Aike Magmatic Province: Active Margin Origin and Implications for the Opening of the Weddell Sea." *Lithos* 386–387: 106013. https://doi.org/10.1016/J.LITHOS.2021.106013.

Beaumont, C. 1981. "Foreland Basins." *Geophysical Journal International* 65, no. 2: 291–329. https://doi.org/10.1111/J.1365-246X.1981.TB02715.X.

Bernet, M., and R. Gaupp. 2005. "Diagenetic History of Triassic Sandstone from the Beacon Supergroup in Central Victoria Land." *New Zealand Journal of Geology and Geophysics* 48, no. 3: 447–458. https://doi.org/10.1080/00288306.2005.9515125.

Berry R. F., and S. W. Bull. 2012. "The Pre-Carboniferous Geology of Tasmania." *Episodes* 35: 195–204.

Berry, R. F., and S. W. Bull. 2012. "The pre-Carboniferous Geology of Tasmania." *Episodes*, 35, 195–204. https://doi.org/10.18814/epiiugs/2012/v35i1/019.

Berry, R., and M. Banks. 1985. "Striations on Minor Faults and the Structure of the Parmeener Super-Group near Hobart, Tasmania." *Papers and Proceedings of The Royal Society of Tasmania* 119: 23–29. https://doi.org/10.26749/rstpp.119.23.

Bishop, B. T., S. L. Beck, G. Zandt, L. S. Wagner, M. D. Long, and H. Tavera. 2018. "Foreland Uplift during Flat Subduction: Insights from the Peruvian Andes and Fitzcarrald Arch." *Tectonophysics* 731–732: 73–84. https://doi.org/10.1016/J.TECTO.2018.03.005.

Boger, S. D. 2011. "Antarctica—Before and after Gondwana." *Gondwana Research : International Geoscience Journal* 19, no. 2: 335–371. https://doi.org/10.1016/j.gr.2010.09.003.

Bomfleur, B., J. Schneider, R. Schöner, L. Viereck-Götte, and H. Kerp. 2011. "Fossil Sites in the Continental Victoria and Ferrar Groups (Triassic Jurassic) of North Victoria Land, Antarctica." *Polarforschung* 80, no. 2: 88–89.

Bomfleur, B., R. Schöner, J. W. Schneider, L. Viereck, H. Kerp, and J. L. McKellar. 2014. "From the Transantarctic Basin to the Ferrar Large Igneous Province-New Palynostratigraphic Age Constraints for Triassic-Jurassic Sedimentation and Magmatism in East Antarctica." *Review of Palaeobotany and Palynology* 207: 18–37. https://doi.org/10.1016/J.REVPALBO.2014.04.002.

Bomfleur, B., T. Mörs, J. Unverfärth, et al. 2021. "Uncharted Permian to Jurassic Continental Deposits in the Far North of Victoria Land, East

11758791, 2026, 1, Downloaded from https://nsrz.onlinelibrary.wiley.com/doi/10.1002/jgo2.70023 by CochraneItalia, Wiley Online Library on [10/03/2026]. See the Terms and Conditions (https://onlinelibrary.wiley.com/terms-and-conditions) on Wiley Online Library for rules of use; OA articles are governed by the applicable Creative Commons License

Antarctica." *Journal of the Geological Society* 178, no. 1. https://doi.org/10.1144/jgs2020-062.

Bradshaw, M. A. 2013. "The Taylor Group (Beacon Supergroup): The Devonian Sediments of Antarctica." *Geological Society, London, Special Publications* 381, no. 1: 67–97. https://doi.org/10.1144/SP381.23.

Brown, A. V., C. R. Calver, K. D. Corbett, et al. 1995, Geological Atlas 1:250 000 Digital Series.

Burgess, S. D., J. D. Muirhead, and S. A. Bowring. 2017. "Initial Pulse of Siberian Traps Sills as the Trigger of the End-Permian Mass Extinction." *Nature Communications* 8, no. 1: 1–6. https://doi.org/10.1038/s41467-017-00083-9.

Calver, C. R., D. J. Mantle, J. L. Crowley, and R. S. Nicoll. 2021. "Triassic Coal Measures, Tasmania: New U–Pb CA-TIMS Ash Bed Dates and Numerical Calibration of Palynostratigraphy." *Australian Journal of Earth Sciences* 68, no. 7: 1005–1016. https://doi.org/10.1080/08120099.2021.1888804.

Calver, C. R., J. L. Everard, and D. J. Mantle, 2023. An Early Triassic Microflora from Schouten Island. Geological Survey Technical Report. 34.

Calver, C. R., P. W. Baillie, M. R. Banks, and D. B. Seymour. 2014. "Ordovician-Lower Devonian Successions." In Geological Evolution of Tasmania, ed. by K. D. Corbett, P. G. Quilty, C. R. Calver, 241–272. Geological Society of Australia.

Campbell, M. J., G. Rosenbaum, C. M. Allen, and N. Mortimer. 2020. "Origin of Dispersed Permian–Triassic fore-Arc Basin Terranes in New Zealand: Insights from Zircon Petrochronology." *Gondwana Research* 78: 210–227. https://doi.org/10.1016/J.GR.2019.08.010.

Capponi, G., C. Montomoli, M. Simonetti, et al. 2024. "A Comprehensive 1: 250,000 Scale Geological Map of the Convoy Range and Franklin Island Quadrangles (Victoria Land, Antarctica)." *Geological Field Trips and Maps* 16, no. 1.5: 1–22. https://doi.org/10.3301/GFT.2024.05.

Capponi, G., L. Crispini, M. Meccheri, G. Musumeci, and P. C. Pertusati. 1999. "Antarctic Geological 1/250000 Map series." Mt. Joyce Quadrangle, (Victoria Land). https://doi.org/10.13140/RG.2.1.3254.9284.

Casnedi, R., and A. Di Giulio. 1999. "Sedimentology of the Section Peak Formation (Jurassic), Northern Victoria Land, Antarctica." In Fluvial Sedimentology, ed. by N. D. Smith and J. Rogers, 435–449. John Wiley & Sons, Ltd. https://doi.org/10.1002/9781444304213.CH30.

Catuneanu, O. 2004. "Retroarc Foreland Systems––evolution through Time." *Journal of African Earth Sciences* 38, no. 3: 225–242. https://doi.org/10.1016/J.JAFREARSCI.2004.01.004.

Clarke, M. J. 1989. "Lower Parmeener Supergroup." In Geological Miner Resource Tasmania, ed. by C. F. Burrett and E.L Martin, 295–309, Geological Society of Australia, Special Publication. vol. 15.

Collinson, J. W. 1990. "Depositional Setting of Late Carboniferous to Triassic Biota in the Transantarctic Basin."Antarct Paleobiol Its role Reconstr Gondwana, ed. byT. N. Taylor and E. L. Taylor, 1–14. Springer.

Collinson, J. W., D. C. Pennington, and N. R. Kemp. 1983. "Sedimentary Petrology of Permian-Triassic Fluvial Rocks in Allan Hills, Central Victoria Land." *Antarctic Journal of United States* 18, no. 5: 20–22.

Collinson, J. W., D. C. Pennington, and N. R. Kemp. 1986. "Stratigraphy and Petrology of Permian and Triassic Fluvial Deposits in Northern Victoria Land, Antarctica." Geology Investigation, ed. by E. Stump. American Geophysical Union (AGU). https://doi.org/10.1002/9781118664957.ch9.

Collinson, J. W., J. L. Isbell, D. H. Elliot, M. F. Miller, J. M. G. Miller, and J. J. Veevers. 1994. "Permian-Triassic Transantarctic Basin." In Permian-Triassic Pangean Basins Foldbelt along Panthalassan Marfin Gondwanal, ed. by J. J. Veevers and C. Powell, 173–222. Veevers, vol. 184. https://doi.org/10.1130/MEM184-p173.

Collinson, J. W., N. R. Kemp, and T. J. Eggert. 1987. "Comparison of Triassic Gondwana Sequences in the Transantarctic Mountains and Tasmania," In Gondwana Six Stratigr Sedimentol Paleontol, ed. by G. D. McKenzie, 51–61. American Geophysical Union (AGU).

Collinson, J., J. Eggert, and N. Kemp. 1990. "Triassic Sandstone Petrology of Tasmania: Evidence for a Tasmania-Transantarctic Basin." *Papers and Proceedings of The Royal Society of Tasmania* 124, no. 1: 61–75. https://doi.org/10.26749/rstpp.124.1.61.

Corbett, K. D., R. F. Berry, J. L. Everard, et al. 2014. "Cambrian Tasmania," In Geological Evolution of Tasmania. ed. by K. D. Corbett, P. G. Quilty, C. R. Calver, 95–240, Geological Society of Australia (Tasmania Division).

Cornamusini, G., F. M. Talarico, S. Cirilli, A. Spina, V. Olivetti, and J. Woo. 2017. "Upper Paleozoic Glacigenic Deposits of Gondwana: Stratigraphy and Paleoenvironmental Significance of a Tillite Succession in Northern Victoria Land (Antarctica)." *Sedimentary Geology* 358: 51–69. https://doi.org/10.1016/j.sedgeo.2017.07.002.

Cornamusini, G., L. Zurli, G. P. Liberato, et al. 2023. "*A Lithostratigraphic Reappraisal of a Permian-Triassic Fluvial Succession at Allan Hills (Antarctica) and Implications for the Terrestrial End-Permian Extinction Event,"Palaeogeography, Palaeoclimatology, Palaeoecology* 627: 111741.

Corti, V., J. Unverfärth, L. Zurli, G. Cornamusini, and B. Bomfleur. 2026. "Palynostratigraphic Age Assessment of Victoria and Ferrar Group Deposits in the Central Prince Albert Mountains, Victoria Land." *New Zealand Journal of Geology and Geophysics* In Review.

Cox, S. C., B. Smith Lyttle, S. Elkind, et al. 2023. "A Continent-Wide Detailed Geological Map Dataset of Antarctica." *Scientific Data* 10, no. 1: 1–14. https://doi.org/10.1038/s41597-023-02152-9.

Cox, S. C., I. M. Turnbull, M. J. Isaac, D. B. Townsend, and B. S. Lyttle. 2012. Geology of Southern Victoria Land Antarctica. Institute. Lower Hutt.

Craddock, J. P., M. D. Schmitz, J. L. Crowley, et al. 2017b. "Precise U-Pb Zircon Ages and Geochemistry of Jurassic Granites, Ellsworth-Whitmore Terrane, Central Antarctica." *Geological Society of America Bulletin* 129, no. 1-2: 118–136. https://doi.org/10.1130/B31485.1.

Craddock, J. P., P. Fitzgerald, A. Konstantinou, A. Nereson, and R. J. Thomas. 2017a. "Detrital Zircon Provenance of Upper Cambrian-Permian Strata and Tectonic Evolution of the Ellsworth Mountains, West Antarctica." *Gondwana Research* 45: 191–207. https://doi.org/10.1016/j.gr.2016.11.011.

Craddock, J. P., R. W. Ojakangas, D. H. Malone, et al. 2019. "Detrital Zircon Provenance of Permo-Carboniferous Glacial Diamictites across Gondwana." *Earth-Science Reviews* 192: 285–316. https://doi.org/10.1016/j.earscirev.2019.01.014.

Criniti, S., M. Martín-Martín, and A. Martín-Algarra. 2023. "New Constraints for the Western Paleotethys Paleogeography-Paleotectonics Derived from Detrital Signatures: Malaguide Carboniferous Culm Cycle (Betic Cordillera, S Spain).." *Sedimentary Geology* 458: 106534. https://doi.org/10.1016/J.SEDGEO.2023.106534.

Criniti, S., M. Martín-Martín, R. Hlila, A. Maaté, and S. Maaté. 2024. "Detrital Signatures of the Ghomaride Culm Cycle (Rif Cordillera, N Morocco): New Constraints for the Northern Gondwana Plate Tectonics." *Marine and Petroleum Geology* 165: 106861. https://doi.org/10.1016/J.MARPETGEO.2024.106861.

Critelli, S. 2018. "Provenance of Mesozoic to Cenozoic Circum-Mediterranean Sandstones in Relation to Tectonic Setting." *Earth-Science Review* 185: 624–648. https://doi.org/10.1016/J.EARSCIREV.2018.07.001.

Critelli, S., F. Perri, J. Arribas, et al. 2022. "Sandstone Detrital Modes and Diagenetic Evolution of Mesozoic Continental Red Beds from

11758791, 2026, 1, Downloaded from https://nzjg.onlinelibrary.wiley.com/doi/10.1002/jgo2.70023 by CochraneItalia, Wiley Online Library on [10/03/2026]. See the Terms and Conditions (https://onlinelibrary.wiley.com/terms-and-conditions) on Wiley Online Library for rules of use; OA articles are governed by the applicable Creative Commons License

Western-Central Circum-Mediterranean Orogenic Belts. Spec Pap Geol Soc Am, Environmental Crises at the Permian–Triassic Mass Extinction." *Nature Reviews. Earth & Environment* 3, no. 3: 119-33-197–214. https://doi.org/10.1038/s43017-021-00259-4.

Critelli, S., S. Criniti, R. V. Ingersoll, and W. Cavazza. 2022. "Temporal and Spatial Significance of Volcanic Particles in Sand(stone): Implications for Provenance and Palaeotectonic Reconstructions." *Geological Society, London, Special Publications* 520, no. 1: 311–325. https://doi.org/10.1144/SP520-2022-99.

Dal Corso, J., H. Song, S. Callegaro, et al. 2022. Environmental Crises at the Permian–Triassic Mass Extinction. *Nature Reviews Earth & Environment*, no. 3: 197–214. https://doi.org/10.1038/s43017-021-00259-4.

Dalziel, I. W. D., and D. H. Elliot. 1982. "West Antarctica: Problem Child of Gondwanaland." *Tectonics* 1, no. 1: 3–19. https://doi.org/10.1029/TC001I001P00003.

Decelles, P. G. 2012. "Foreland Basin Systems Revisited: Variations in Response to Tectonic Settings." In Tectonics of Sedimentary Basins Recent Advances, ed. by C. Busby and A. Azor, 405–426. John Wiley & Sons, Ltd. https://doi.org/10.1002/9781444347166.CH20.

DeCelles, P. G., and K. A. Giles. 1996. "Foreland Basin Systems." *Basin Research* 8, no. 2: 105–123. https://doi.org/10.1046/J.1365-2117.1996.01491.X.

Di Giulio, A., P. Sternai, R. Sacchi, and L. Castrogiovanni. 2026. "Geodynamic Pacemaker of Phanerozoic Climate: A Multivariate Analysis of Plate Boundary Processes and Global Temperature Variations." *Global and Planetary Change* 256: 105173. https://doi.org/10.1016/j.gloplacha.2025.105173.

Di Giulio, A., R. Tribuzio, A. Ceriani, and M. Riccardi. 1999. "Integrated Analyses Constraining the Provenance of Sandstones, a Case Study: The Section Peak Formation (Beacon Supergroup, Antarctica)." *Sedimentary Geology* 124, no. 1–4: 169–183. https://doi.org/10.1016/S0037-0738(98)00126-2.

Elliot, D. H. 1996. "The Hanson Formation: A New Stratigraphical Unit in Transantarctic Mountains, Antarctica." *Antarctic Science* 8: 389–394.

Elliot, D. H. 2013. "The Geological and Tectonic Evolution of the Transantarctic Mountains: A Review." *Geological Society, London, Special Publications* 381, no. 1: 7–35. https://doi.org/10.1144/SP381.14.

Elliot, D. H. 2024. "Nilsen Plateau, Transantarctic Mountains, Antarctica: An Update on the Gondwana Stratigraphy and Structure." *New Zealand Journal of Geology and Geophysics* 68: 1–1258. https://doi.org/10.1080/00288306.2024.2407132.

Elliot, D. H., and C. G. Grimes. 2011. "Triassic and Jurassic Strata at Coombs Hills, South Victoria Land: Stratigraphy, Petrology and Cross-Cutting Breccia Pipes." *Antarctic Science* 23, no. 3: 268–280. https://doi.org/10.1017/S0954102010000994.

Elliot, D. H., and C. M. Fanning. 2008. "Detrital Zircons from Upper Permian and Lower Triassic Victoria Group Sandstones, Shackleton Glacier Region, Antarctica: Evidence for Multiple Sources along the Gondwana Plate Margin." *Gondwana Research* 13, no. 2: 259–274. https://doi.org/10.1016/j.gr.2007.05.003.

Elliot, D. H., and T. H. Fleming. 2021. "Ferrar Large Igneous Province: Petrology," In Volcanism Antarct 200 Million Years Subduction, ed. by J. L. Smellie, K. S. Panter and A. Geyer, 93–119, Rift Cont Break. Vol. 55, https://doi.org/10.1144/M55-2018-39.

Elliot, D. H., C. M. Fanning, and S. R. W. Hulett. 2015. "Age Provinces in the Antarctic Craton: Evidence from Detrital Zircons in Permian Strata from the Beardmore Glacier Region, Antarctica." *Gondwana Research* 28, no. 1: 152–164. https://doi.org/10.1016/j.gr.2014.03.013.

Elliot, D. H., C. M. Fanning, and T. S. Laudon. 2016. "The Gondwana Plate Margin in the Weddell Sea Sector: Zircon Geochronology of Upper Paleozoic (mainly Permian) Strata from the Ellsworth Mountains and Eastern Ellsworth Land, Antarctica." *Gondwana Research* 29, no. 1: 234–247. https://doi.org/10.1016/j.gr.2014.12.001.

Elliot, D. H., C. M. Fanning, J. L. Isbell, and S. R. W. Hulett. 2017a. "The Permo-Triassic Gondwana Sequence, Central Transantarctic Mountains, Antarctica: Zircon Geochronology, Provenance, and Basin Evolution." *Geosphere* 13, no. 1: 155–178. https://doi.org/10.1130/GES01345.1.

Elliot, D. H., C. M. Fanning, S. B. Mukasa, and I. L. Millar. 2019. "Hf- and O-Isotope Data from Detrital and Granitoid Zircons Reveal Characteristics of the Permian–Triassic Magmatic Belt along the Antarctic Sector of Gondwana." *Geosphere* 15, no. 2: 576–604. https://doi.org/10.1130/GES02011.1.

Elliot, D. H., D. Larsen, C. M. Fanning, T. H. Fleming, and J. D. Vervoort. 2017b. "The Lower Jurassic Hanson Formation of the Transantarctic Mountains: Implications for the Antarctic Sector of the Gondwana Plate Margin." *Geological Magazine* 154, no. 4: 777–803. https://doi.org/10.1017/S0016756816000388.

Elsner, M. 2010. Triassic to Early Jurassic Sandstones in North Victoria Land, Antarctica: Composition, Provenance, and Diagenesis. Friedrich-Schiller-Universität.

Elsner, M., R. Schöner, A. Gerdes, and R. Gaupp. 2013. "Reconstruction of the Early Mesozoic Plate Margin of Gondwana by U–Pb Ages of Detrital Zircons from Northern Victoria Land, Antarctica." *Geological Society, London, Special Publications* 383, no. 1: 211–232. https://doi.org/10.1144/SP383.5.

Farabee, M.J.,T.N. Taylor, and E.L. Taylor. 1989. Pollen and Spore Assemblages from the Falla Formation (Upper Triassic), Central Transantarctic Mountains, Antarctica. *Review of Palaeobotany and Palynology* 61, no. 1–2: 101–138. https://doi.org/10.1016/0034-6667(89)90065-1.

Fielding, C. R., T. D. Frank, J. L. Isbell, L. C. Henry, and E. W. Domack. 2010. "Stratigraphic Signature of the Late Paleozoic Ice Age in the Parmeener Supergroup of Tasmania, SE Australia, and Inter-Regional Comparisons." *Palaeogeography, Palaeoclimatology, Palaeoecology* 298, no. 1–2: 70–90. https://doi.org/10.1016/j.palaeo.2010.05.023.

Fielding, C. R., T. D. Frank, L. P. Birgenheier, M. C. Rygel, A. T. Jones, and J. Roberts. 2008. "Stratigraphic Imprint of the Late Paleozoic Ice Age in Eastern Australia: A Record of Alternating Glacial and Nonglacial Climate Regime." *Journal of the Geological Society* 165, no. 1: 129–140. https://doi.org/10.1144/0016-76492007-036.

Fielding, C. R., T. D. Frank, S. McLoughlin, et al. 2019. "Age and Pattern of the Southern High-Latitude Continental End-Permian Extinction Constrained by Multiproxy Analysis." *Nature Communications* 10, no. 1: 1–12. https://doi.org/10.1038/s41467-018-07934-z.

Forsyth, S. 1989. Upper Parmeener Supergroup. in: Geol Miner Resour Tasmania. Geological Society of Australia Special Publication, 308–333.

Gazzi, P. 1966. "Le Arenanarie Del Flysh Sopracretaceo Dell'Appennino Modenese: Correlazioni Con il Flysh Di Monghidoro,"*Mineral Petrographica Acta* 12: 69–97.

Glen, R. A., and R. A. Cooper. 2021. "Evolution of the East Gondwana Convergent Margin in Antarctica, Southern Australia and New Zealand from the Neoproterozoic to Latest Devonian." *Earth-Science Review* 220: 103687. https://doi.org/10.1016/J.EARSCIREV.2021.103687.

Goodge, J. W. 2020. "Geological and Tectonic Evolution of the Transantarctic Mountains, from Ancient Craton to Recent Enigma." *Gondwana Research* 80: 50–122. https://doi.org/10.1016/j.gr.2019.11.001.

Goodge, J. W., and C. M. Fanning. 2010. "Composition and Age of the East Antarctic Shield in Eastern Wilkes Land Determined by Proxy from Oligocene-Pleistocene Glaciomarine Sediment and Beacon Supergroup Sandstones, Antarctica." *Geological Society of America Bulletin* 122, no. 7-8: 1135–1159. https://doi.org/10.1130/B30079.1.

11758791, 2026, 1, Downloaded from https://nzrc.onlinelibrary.wiley.com/doi/10.1002/jgo2.70023 by CochraneItalia, Wiley Online Library on [10/03/2026]. See the Terms and Conditions (https://onlinelibrary.wiley.com/terms-and-conditions) on Wiley Online Library for rules of use; OA articles are governed by the applicable Creative Commons License

Graham, S. A., R. B. Tolson, P. G. Decelles, et al. 1986. "Provenance Modeling as a Technique for Analyzing Source Terrane Evolution and Controls on Foreland Sedimentation." ed. by P. A. Allen and P. Homewood, 425–436). John Wiley & Sons, Ltd., https://doi.org/10.1002/9781444303810.CH23.

Gulbranson, E. L., G. Cornamusini, P. E. Ryberg, and V. Corti. 2020. "When Does Large Woody Debris Influence Ancient Rivers? Dendrochronology Applications in the Permian and Triassic, Antarctica." *Palaeogeogr Palaeoclimatol Palaeoecol* 541: 109544. https://doi.org/10.1016/j.palaeo.2019.109544.

Gunner, J. 1971. "Ida Granite: A New Formationof the Granite Harbor Intrusives, Beardmore Glacier Region." *Antarctic Journal of United States* 6: 194–196.

Hand, S. J. 1993. "Paleogeography of Tasmania's Permo-Carboniferous Glacigenic Sediments." In Gondwana Eight Assem Evol Dispersal, ed. by R. H. Findlay, R. Unrug, M. R. Banks, J. J. Veevers, and A. A. Balkema (CRC Press) 459–469.

Henjes-Kunst, F., and H. Kreuzer. 2003. "Mid-Paleozoic Igneous Activity in Northern Victoria Land, Antarctica: Implications of New Geochronological Data." *Geological Society* 85: 271–302.

Henry, L. C., J. L. Isbell, C. R. Fielding, E. W. Domack, T. D. Frank, and M. L. Fraiser. 2012. "Proglacial Deposition and Deformation in the Upper Carboniferous to Lower Permian Wynyard Formation, Tasmania: A Process Analysis." *Palaeogeography, Palaeoclimatology, Palaeoecology* 315-316: 142–157. https://doi.org/10.1016/j.palaeo.2011.11.020.

Horton, B. K. 2022. "Unconformity Development in Retroarc Foreland Basins: Implications for the Geodynamics of Andean-Type Margins." *Journal of the Geological Society* 179, no. 3, https://doi.org/10.1144/JGS2020-263/ASSET/B4BA5FDF-FEB6-4038-BF9B-E403996304C7/ASSETS/IMAGES/LARGE/JGS2020-263.09.JPG.

Horton, B. K., T. N. Capaldi, C. Mackaman-Lofland, et al. 2022. "Broken Foreland Basins and the Influence of Subduction Dynamics, Tectonic Inheritance, and Mechanical Triggers." *Earth-Science Review* 234: 104193. https://doi.org/10.1016/J.EARSCIREV.2022.104193.

Ingersoll, RV., T. F. Bullard, R. L. Ford, J. P. Grimm, J. D. Pickle, and S. W. Sares. 1984. "The Effect of Grain Size on Detrital Modes: A Test of the Gazzi-Dickinson Point-Counting Method." *Journal of Sedimentary Research* 54, no. 1: 103–116. https://doi.org/10.1306/212F83B9-2B24-11D7-8648000102C1865D.

Isbell, J. L. 2010. "Environmental and Paleogeographic Implications of Glaciotectonic Deformation of Glaciomarine Deposits Within Permian Strata of the Metschel Tillite, Southern Victoria Land, Antarctica. in: Late Paleoz Glacial Events Postglacial Transgressions Gondwana [Internet]." *Geological Society of America* 468: 81–100. https://doi.org/10.1130/2010.2468(03).

Isbell, J. L., and N. R. Cúneo. 1996. "Depositional Framework of Permian Coal-Bearing Strata, Southern Victoria Land, Antarctica." *Palaeogeography, Palaeoclimatology, Palaeoecology* 125, no. 1–4: 217–238. https://doi.org/10.1016/S0031-0182(96)00032-6.

Isbell, J. L., G. A. Gelhar, and G. M. Seegers. 1997. "Reconstruction off Preglacial Topography Using a Postglacial Flooding Surface; Upper Paleozoic Deposits, Central Transantarctic Mountains, Antarctica." *Journal of Sedimentary Research* 67, no. 2: 264–273. https://doi.org/10.1306/D426854A-2B26-11D7-8648000102C1865D.

Isbell, J. L., L. C. Henry, E. L. Gulbranson, et al. 2012. "Glacial Paradoxes during the Late Paleozoic Ice Age: Evaluating the Equilibrium Line Altitude as a Control on Glaciation." *Gondwana Research* 22, no. 1: 1–19. https://doi.org/10.1016/j.gr.2011.11.005.

Isbell, J. L., Z. J. Koch, G. M. Szablewski, and P. A. Lenaker 2008. "Permian Glacigenic Deposits in the Transantarctic Mountains, Antarctica." In Special Paper 441: Resolving the Late Paleozoic Ice Age in Time and Space. 59–70, Geological Society of America, Vol. 441.https://doi.org/10.1130/2008.2441(04).

Ives, L. R. W., and J. L. Isbell. 2021. "A Lithofacies Analysis of a South Polar Glaciation in the Early Permian: Pagoda Formation, Shackleton Glacier Region, Antarctica." *Journal of Sedimentary Research* 91, no. 6: 611–635. https://doi.org/10.2110/jsr.2021.004.

Ives, L. R. W., and J. L. Isbell. 2023. "Lithofacies and Sequence Stratigraphic Analysis of the Glaciomarine Lower Wynyard Formation (Pennsylvanian–early Permian, Tasmanian Basin." *Sedimentary Geology* 455: 106482. https://doi.org/10.1016/j.sedgeo.2023.106482.

Ives, L. R. W., J. L. Isbell, and K. J. Licht. 2022. "A "Local First" Approach to Glacigenic Sediment Provenance Demonstrated Using U-Pb Detrital Zircon Geochronology of the Permo-Carboniferous Wynyard Formation, Tasmanian Basin." *Sedimentary Record* 20, no. 1: https://doi.org/10.2110/001C.38180.

John, N. 2014. "Sedimentology and Composition of the Takrouna Formation, Northern Victoria Land, Antarctica - Provenance and Depositional Evolution of a Permian Gondwana Basin, the Geological History and Evolution of West Antarctica," In Nature Reviews Earth & Environment, 117–133. University of Jena, vol. 1, 2, Jordan TA, Riley TR, Siddoway CS. 2020. https://doi.org/10.1038/s43017-019-0013-6.

Jordan, T. E., P. B. Flemings, and J. A. Beer. 1988. "Dating Thrust-Fault Activity by Use of Foreland-Basin Strata." In Frontiers in Sedimentary Geology, ed. by K. L. Kleinspehn and C. Paola, 307–330. Springer, https://doi.org/10.1007/978-1-4612-3788-4_16.

Jordan, T. A., T. R. Riley, C. S. Siddoway, 2020. The Geological History and Evolution of West Antarctica. Nature Reviews Earth & Environment *Nature Rev. Earth & Environ*. 1, 117–133. https://doi.org/10.1038/s43017-019-0013-6.

Kim, D., S.-B. Yi, H. Kim, K. Taehwan, K. Taehoon, and J. I. Lee. 2021. "Geochemistry and Geochronology of Early Paleozoic Intrusive Rocks in the Terra Nova Bay Area, Northern Victoria Land, Antarctica." *Minerals* 11, no. 7: 787. https://doi.org/10.3390/min11070787.

Koch, Z. J., and J. L. Isbell. 2013. "Processes and Products of Grounding-Line Fans from the Permian Pagoda Formation, Antarctica: Insight into Glacigenic Conditions in Polar Gondwana." *Gondwana Research* 24, no. 1: 161–172. https://doi.org/10.1016/j.gr.2012.10.005.

Korsch, R. J. 1974. "Petrographic Comparison of the Taylor and Victoria Groups (Devonian to Triassic) in South Victoria Land, Antarctica." *New Zealand Journal of Geology and Geophysics* 17, no. 3: 523–541. https://doi.org/10.1080/00288306.1973.10421579.

Kreuzer, H., A. HöHndorf, H. Lenz, P. MüLler, and U. Vetter. 1987. "Radiometric Ages of Pre-Mesozoic Rocks from Northern Victoria Land, Antarctica." In Gondwana Six Struct Tectonics Geophys, ed. by G. D. McKenzie, 31–47, https://doi.org/10.1029/GM040p0031.

Laird, M. G., and J. D. Bradshaw, 1981. "Permian Tillites of North Victoria Land," In Earth's Pre-Pleistocene Glacial Record, ed. by M. J. Hambrey and W. B. Harland, 237–240.Cambridge University Press.

Lisker, F., A. L. Läufer, M. Olesch, F. Rossetti, and T. Schäfer. 2006. "Transantarctic Basin: New Insights from Fission Track and Structural Data from the USARP Mountains and Adjacent Areas (Northern Vicoria Land, Antarctica)." *Basin Research* 18, no. 4: 497–520. https://doi.org/10.1111/J.1365-2117.2006.00301.X.

McBride, E. F. 1963. "A Classification of Common Sandstones." *Journal of Sedimentary Research* 33, no. 3: 664–669. https://doi.org/10.1306/74D70EE8-2B21-11D7-8648000102C1865D.

McKelvey B. C., P. N. Webb, & B. P. Kohn, 1977. Stratigraphy of the Taylor and Lower Victoria Groups (Beacon Supergroup) between the Mackay Glacier and Boomerang Range, Antarctica. *New Zealand Journal of Geology and Geophysics* 20, no. 5: 813–863. https://doi.org/10.1080/00288306.1977.10420685.

11758791, 2026, 1, Downloaded from https://nzrc.onlinelibrary.wiley.com/doi/10.1002/jgo2.70023 by CochraneItalia, Wiley Online Library on [10/03/2026]. See the Terms and Conditions (https://onlinelibrary.wiley.com/terms-and-conditions) on Wiley Online Library for rules of use; OA articles are governed by the applicable Creative Commons License

McPherson, J. G. 1975. The Aztec Siltstone: an Upper Devonian Alluvial Plain Red Bed Sequence. Victoria University of Wellington. https://doi.org/10.26686/wgtn.16945582.v1.

McPherson, J. G. 1978. "Stratigraphy and Sedimentology of the Upper Devonian Aztec Siltstone, Southern Victoria Land, Antarctica." *New Zealand Journal of Geology and Geophysics* 21, no. 6: 667–683. https://doi.org/10.1080/00288306.1978.10425198.

Merdith, A. S., S. E. Williams, A. S. Collins, et al. 2021. "Extending Full-Plate Tectonic Models into Deep Time: Linking the Neoproterozoic and the Phanerozoic." *Earth-Science Review* 214: 103477. https://doi.org/10.1016/J.EARSCIREV.2020.103477.

Mitrovica, J. X., C. Beaumont, and G. T. Jarvis. 1989. "Tilting of Continental Interiors by the Dynamical Effects of Subduction." *Tectonics* 8, no. 5: 1079–1094. https://doi.org/10.1029/TC008I005P01079.

Morlighem, M. 2020. MEaSUREs BedMachine Antarctica, Version 2. Boulder, Color USA NASA Natl Snow Ice Data Cent Distrib Act Arch Cent.. https://doi.org/https://doi.org/10.5067/E1QL9HFQ7A8M.

Morlighem, M., E. Rignot, T. Binder, et al. 2020. "Deep Glacial Troughs and Stabilizing Ridges Unveiled beneath the Margins of the Antarctic Ice Sheet." *Nature Geoscience* 13, no. 2: 132–137. https://doi.org/10.1038/s41561-019-0510-8 2019.

Müller, C., J. Elliott, T. A. M. Pugh, et al. 2018. "Global Patterns of Crop Yield Stability under Additional Nutrient and Water inputs.Gonzalez." *PLoS One* 13, no. 6: e0198748. https://doi.org/10.1371/journal.pone.0198748.

Navarrete, C., G. Gianni, A. Encinas, et al. 2019. "Triassic to Middle Jurassic Geodynamic Evolution of Southwestern Gondwana: From a Large Flat-Slab to Mantle Plume Suction in a Rollback Subduction Setting." *Earth-Science Review* 194: 125–159. https://doi.org/10.1016/j.earscirev.2019.05.002.

Nelson, D. A., and J. M. Cottle. 2018. "The Secular Development of Accretionary Orogens: Linking the Gondwana Magmatic Arc Record of West Antarctica, Australia and South America." *Gondwana Research* 63: 15–33. https://doi.org/10.1016/J.GR.2018.06.002.

Norris, G. 1965. "Triassic and Jurassic Miospores and Acritarchs from the Beacon and Ferrar Groups, Victoria Land, Antarctica." *New Zealand Journal of Geology and Geophysics* 8: 236–277.

Olivetti, V., L. Zurli, S. Cattò, et al. 2026. "Late Paleozoic-Mesozoic Uplift, Exhumation, and Burial of Southern Gondwana Margin: Thermochronological and Stratigraphic Constrains from Victoria Land (Antarctica)." *Gondwana Research*. https://doi.org/10.1016/j.gr.2025.12.003.

Pankhurst, R. J., I. L. Millar, A. M. Grunow, and B. C. Storey. 1993. "The Pre-Cenozoic Magmatic History of the Thurston Island Crustal Block, West Antarctica." *Journal of Geophysical Research: Solid Earth* 98, no. B7: 11835–11849. https://doi.org/10.1029/93JB01157.

Pankhurst, R. J., S. D. Weaver, J. D. Bradshaw, B. C. Storey, and T. R. Ireland. 1998. "Geochronology and Geochemistry of Pre-Jurassic Superterranes in Marie Byrd Land, Antarctica." *Journal of Geophysical Research: Solid Earth* 103, no. B2: 2529–2547. https://doi.org/10.1029/97JB02605.

Paulsen, T., C. Deering, J. Sliwinski, O. Bachmann, and M. Guillong. 2017a. "New Detrital Zircon Age and Trace Element Evidence for 1450 Ma Igneous Zircon Sources in East Antarctica." *Precambrian Research* 300: 53–58. https://doi.org/10.1016/j.precamres.2017.07.011.

Paulsen, T., C. Deering, J. Sliwinski, V. Valencia, O. Bachmann, and M. Guillong. 2017b. "Detrital Zircon Ages and Trace Element Compositions of Permian–Triassic Foreland Basin Strata of the Gondwanide Orogen, Antarctica." *Geosphere* 13, no. 6: 2085–2093. https://doi.org/10.1130/GES01482.1.

Paulsen, T., J. Benowitz, S. Thomson, et al. 2025. "Antarctic Phanerozoic Landscape Evolution along the Transantarctic Basin from Thermochronology." *Earth and Planetary Science Letters* 664: 119445. https://doi.org/10.1016/j.epsl.2025.119445.

Pertusati, P. C., C. Ribecai, R. Carosi, and M. Meccheri. 2006. "Early Jurassic Age for Youngest Beacon Supergroup Strata Based on Palynomorphs from Section Peak, Northern Victoria Land, Antarctica." *Terra Antarctic* 12: 99–104.

Reid, C. M., S. M. Forsyth, M. J. Clarke, and C. Bacon. 2014. The Parmeener Supergroup - Late Carboniferous to Triassic, ed. by K. D. Corbett, P. G. Quilty, and C. R. Calver, 363–384, Geological Evolution Tasmania. vol. 24.

Retallack, G. J., A. H. Jahren, N. D. Sheldon, R. Chakrabarti, C. A. Metzger, and R. M. H. Smith. 2005. "The Permian–Triassic Boundary in Antarctica." *Antarctic Science* 17, no. 2: 241–258. https://doi.org/10.1017/S0954102005002658.

Riley, T. R., I. L. Millar, A. Carter, et al. 2023. Evolution of an Accretionary Complex (LeMay Group) and Terrane Translation in the Antarctic Peninsula. *Tectonics*, 42, no. 2: e2022TC007578. https://doi.org/10.1029/2022tc007578.

Schöner, R., and N. John. 2014. "Sedimentological Field Investigations on the Takrouna Formation (Permian, Beacon Supergroup) in Northern Victoria Land, Antarctica." *Polarforschung* 84: 49–58.

Schöner, R., B. Bomfleur, J. W. Schneider, and L. Viereck-Götte. 2011. "Systematic Description of the Triassic to Lower Jurassic Section Peak Formation in North Victoria Land (Antarctica)." *Polarforschung* 80, no. 2: 71–87.

Seymour, D. B., M. P. McClenaghan, G. R. Green, et al. 2014. "Mid-Paleozoic Orogenesis, Magmatism and Mineralisation," In Geological Evolution Tasmania. Geological, ed. by K. D. Corbett, P. G. Quilty, and C. R. Calver, 273–362.Geological Society of Australia.

Sidor, C. A., J. A. McIntosh, B. M. Gee, et al. 2023. "The Fremouw Formation of Antarctica: Updated Vertebrate Fossil Record and Reevaluation of High-Latitude Permian–Triassic Paleoenvironments." *Earth-Science Review* 246: 104587. https://doi.org/10.1016/J.EARSCIREV.2023.104587.

Sirevaag, H., A. Ksienzyk, J. Jacobs, I. Dunkl, and A. Läufer. 2018. "Tectono-Thermal Evolution and Morphodynamics of the Central Dronning Maud Land Mountains, East Antarctica, Based on New Thermochronological Data." *Geosciences* 8, no. 11: 390. https://doi.org/10.3390/geosciences8110390.

Stacey, A. R., and R. F. Berry, 2004. "The Structural History of Tasmania: A Review for Petroleum Explorers. in: East Aust Basin Symp II.

Svensen, H., S. Planke, A. G. Polozov, et al. 2009. "Siberian Gas Venting and the End-Permian Environmental Crisis." *Earth and Planetary Science Letters* 277, no. 3-4: 490–500. https://doi.org/10.1016/J.EPSL.2008.11.015.

Talarico, F., C. Ghezzo, and G. Kleinschmidt. 2022. "The Antarctic Continent in Gondwana: A Perspective from the Ross Embayment and Potential Research Targets for Future Investigations," In Antarctic Climate Evolution, ed. by F. Florindo, M. Siegert and T. R. Naish, 219–296. 2nd. Elsevier. https://doi.org/10.1016/B978-0-12-819109-5.00004-9.

Unverfärth, J., T. Mörs, and B. Bomfleur. 2020. "Palynological Evidence Supporting Widespread Synchronicity of Early Jurassic Silicic Volcanism Throughout the Transantarctic Basin." *Antarctic Science* 32, no. 5: 396–397. https://doi.org/10.1017/S0954102020000346.

Veevers, J. J., P. J. Conaghan, and C. M. Powell. 1994. "Eastern Australia. in: Permian–Triassic Pangean Basins Fold Belts along Panthalassan Margin Gondwanaland." In Geological Society of America Memoirs, ed. by J. J. Veevers and C. M. Powell, Geological Society of America 11–171. vol.184.

Vermeesch, P. 2013. "Multi-Sample Comparison of Detrital Age Distributions." *Chemical Geology* 341: 140–146. https://doi.org/10.1016/J.CHEMGEO.2013.01.010.

11758791, 2026, 1, Downloaded from https://nzjg.onlinelibrary.wiley.com/doi/10.1002/jgo2.70023 by CochraneItalia, Wiley Online Library on [10/03/2026]. See the Terms and Conditions (https://onlinelibrary.wiley.com/terms-and-conditions) on Wiley Online Library for rules of use; OA articles are governed by the applicable Creative Commons License

Vermeesch, P., A. Resentini, and E. Garzanti. 2016. An R Package for Statistical Provenance Analysis. *Sedimentary Geology*.336, 14–25 http://dx.doi.org/10.1016/j.sedgeo.2016.01.009.

Vermeesch, P., and E. Garzanti. 2015. "Making Geological Sense of 'Big Data' in Sedimentary Provenance Analysis." *Chemical Geology*. 409: 20–27.

Walker, B. C. 1980. The Petrology of the Triassic Strata at Horseshoe Mountain. Victoria University of Wellington.

Woolfe, K. J., and P. J. Barrett. 1995. "Constraining the Devonian to Triassic Tectonic Evolution of the Ross Sea Sector." *Terra Antartic* 2, no. 1: 7–21.

Yakymchuk, C., C. R. Brown, M. Brown, C. S. Siddoway, C. M. Fanning, and F. J. Korhonen. 2015. "Paleozoic Evolution of Western Marie Byrd Land, Antarctica." *Geological Society of America Bulletin* 127, no. 9-10: 1464–1484. https://doi.org/10.1130/B31136.1.

Zhang, Q., L. Qiu, D. P. Yan, et al. 2025. "Impact of Slab Rollback on the Surface of Overriding Plate: Late Cretaceous Extension and Topographic Evolution to the West of the Xuefeng Orogen in the South China Block." *Tectonics* 44, no. 3: e2024TC008354. https://doi.org/10.1029/2024TC008354.

Zurli, L. 2018. Caratterizzazione e Studio Di Provenienza Di Successioni Glacigeniche Tardo-Paleozoiche Del Beacon Supergroup in Terra Vittoria (Antartide): Stratigrafia, Petrografia e Geocronologia. University of Siena.

Zurli, L., G. Cornamusini, G. P. Liberato, and P. Conti. 2022a. "New Data on the Late Paleozoic Ice Age Glaciomarine Successions from Tasmania (SE Australia)." *Palaeogeography, Palaeoclimatology, Palaeoecology* 604: 111210.https://doi.org/10.1016/J.PALAEO.2022.111210.

Zurli, L., G. Cornamusini, J. Woo, et al. 2022b. "Detrital Zircons from Late Paleozoic Ice Age Sequences in Victoria Land (Antarctica): New Constraints on the Glaciation of Southern Gondwana." *GSA Bulletin* 134, no. 1-2: 160–178. https://doi.org/10.1130/B35905.1.

Zurli, L., G. P. Liberato, M. Perotti, J. Woo, M. J. Lee, and G. Cornamusini. 2024a. "A Multi-Proxy Detrital Study from Permian-Triassic Fluvial Sequences of Victoria Land (Antarctica): Implications for the Gondwanan Basin Evolution." *Palaeogeography, Palaeoclimatology, Palaeoecology* 641: 112113. https://doi.org/10.1016/J.PALAEO.2024.112113.

Zurli, L., M. Perotti, and G. Cornamusini. 2024b. "Composition of Late Paleozoic Ice Age Tillites in Victoria Land (Antarctica): Implications for Sediment Provenance and Ice Centers Extent in Southern Gondwana." *Rendiconti Online della Società Geologica Italiana* 63: 1–8. https://doi.org/10.3301/ROL.2024.27.

Supporting Information

Additional supporting information can be found online in the Supporting Information section.

11758791, 2026, 1, Downloaded from https://nsrz.onlinelibrary.wiley.com/doi/10.1002/jgo2.70023 by CochraneItalia, Wiley Online Library on [10/03/2026]. See the Terms and Conditions (https://onlinelibrary.wiley.com/terms-and-conditions) on Wiley Online Library for rules of use; OA articles are governed by the applicable Creative Commons License